

SSN 217

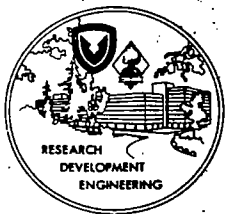
HDL-TR-1737

TR1737-Nuclear Electromagnetic Pulse Simulation by Point Source Injection Techniques for Shielded and Unshielded Penetrations—by Robert F. Gray

Nuclear Electromagnetic Pulse Simulation by Point Source Injection Techniques for Shielded and Unshielded Penetrations

December 1975

THIS RESEARCH WAS SPONSORED BY THE DEFENSE NUCLEAR AGENCY
UNDER SUBTASK R99QAXEB075-43, WORK UNIT 41,
WORK UNIT TITLE "EMP PROGRAM."



U.S. Army Materiel Command
HARRY DIAMOND LABORATORIES
Adelphi, Maryland 20783



INTERACTION BETWEEN THE DISCUS SIMULATOR AND A BURIED WIRE OR PLATE

J. A. Marks

The Dikewood Corporation
1613 University Boulevard, N.E.
Albuquerque, New Mexico 87106

May 1981

Technical Note

Distribution limited to US Government agencies only, because test and evaluation of military systems/equipment are discussed in the report; Feb 80. Other requests for this document must be referred to AFWL/NTYE, Kirtland Air Force Base, NM 87117.

AIR FORCE WEAPONS LABORATORY
Air Force Systems Command
Kirtland Air Force Base, NM 87117

REPORT DOCUMENTATION PAGE		READ INSTRUCTIONS BEFORE COMPLETING FORM
1. REPORT NUMBER AFWL-NTYE-TN-81-15	2. GOVT ACCESSION NO.	3. RECIPIENT'S CATALOG NUMBER
4. TITLE (and Subtitle) INTERACTION BETWEEN THE DISCUS SIMULATOR AND A BURIED WIRE OR PLATE		5. TYPE OF REPORT & PERIOD COVERED Technical Note
		6. PERFORMING ORG. REPORT NUMBER DC-TN-1508-7
7. AUTHOR(s) J. A. Marks		8. CONTRACT OR GRANT NUMBER(s) F29601-79-C-0036
9. PERFORMING ORGANIZATION NAME AND ADDRESS The Dikewood Corporation 1613 University Boulevard, N.E. Albuquerque, New Mexico 87106		10. PROGRAM ELEMENT, PROJECT, TASK AREA & WORK UNIT NUMBERS 64312F/WDNE0716
11. CONTROLLING OFFICE NAME AND ADDRESS Air Force Weapons Laboratory (NTYET) Air Force Systems Command Kirtland AFB, New Mexico 87117		12. REPORT DATE May 29, 1981
		13. NUMBER OF PAGES
14. MONITORING AGENCY NAME & ADDRESS (if different from Controlling Office)		15. SECURITY CLASS. (of this report) UNCLASSIFIED
		15a. DECLASSIFICATION/DOWNGRADING SCHEDULE
16. DISTRIBUTION STATEMENT (of this Report) Distribution limited to US Government agencies only, because test and evaluation of military systems/equipment are discussed in the report; Feb 80. Other requests for this document must be referred to AFWL/NTYE, Kirtland Air Force Base, NM 87117.		
17. DISTRIBUTION STATEMENT (of the abstract entered in Block 20, if different from Report)		
18. SUPPLEMENTARY NOTES		
19. KEY WORDS (Continue on reverse side if necessary and identify by block number) Electromagnetic Scattering Numerical EMP Simulation Radiated EMP Source Region Interaction Three-Dimensional Finite Difference		
20. ABSTRACT (Continue on reverse side if necessary and identify by block number) This report describes the method and results for a three- dimensional finite difference study of the interaction and coupl- ing between a DISCUS type EMP simulator and various buried conductors. The DISCUS arrangement of pulsers simulates the passing EMP from a nuclear surface burst. Various pulser arrangements are considered.		

CONTENTS

<u>Section</u>		<u>Page</u>
I	INTRODUCTION	5
II	GEOMETRY AND MESH	8
III	SOURCE DESCRIPTION	10
IV	RESULTS	11
	1. CASE 1: $\alpha = 1$, 37 m WIRE, 8 m SLATS, DX = 1, 19 PULSERS	12
	2. CASE 2: $\alpha = 2$, 29 m WIRE, 8 m SLATS, DX = 1, 19 PULSERS	13
	3. COMPARISON 1: 2 m VS. 8 m LONG SLATS	13
	4. COMPARISON 2: 9 PULSERS VS. 19 PULSERS	14
	5. COMPARISON 3: PULSER AND WIRE CURRENTS WITH/WITHOUT GROUND RODS ATTACHED TO END PLATE	15
	6. COMPARISON 4: 29 m BARE WIRE WITH OPEN TERMINATION COMPARED TO 54 m BARE WIRE SHORTED TO GROUND RODS	15
	7. COARSE MESH DISCUS CALCULATIONS TO 3 μ s FOR A BURIED UNINSULATED WIRE	16
	a. Slat length variations and environment effects	18
	b. Centered/off centered wire dirve and slat length effects	18
	c. Ground conductivity and pulser position effects	18
V	CONCLUSIONS	20

ILLUSTRATIONS

<u>Figure</u>		<u>Page</u>
1	DISCUS geometry with 1 m mesh	23
2	Source electric field	24
3	Top view (x,y) of E_x , E_y , and E_z mesh point locations for DX slats with slat length = 2 DY	25
4	Slat/pulser/wire mesh point locations (37 m wire, 8 m slats, DX = 1)	26
5	Pulser current and wire current along length of simulator	27
6	Currents at pulser no. 2 (source end, 9 m)	28
7	Currents at pulser no. 10 (center, 25 m)	29
8	Currents at pulser no. 18 (far end, 41 m)	30
9	Slat/pulser/wire mesh point locations (29 m wire, 8 m slats, DX = 1)	31
10	Electric fields normal to 29 m wire	32
11	Wire current and normal electric fields 2 m from source end	33
12	Wire current and normal electric fields at midpoint of 29 m wire	34
13	Wire current and normal electric fields 2 m from far end	35
14	Pulser current and wire current along length of simulator	36
15	$\alpha = 2$, 29 m wire, 8 m slats, DX = 1, 19 pulsers, OBS-1	37
16	$\alpha = 2$, 29 m wire, 8 m slats, DX = 1, 19 pulsers, OBS-4 (midpoint)	38
17	$\alpha = 2$, 29 m wire, 8 m slats, DX = 1, 19 pulsers, OBS-7	39
18	Slat/pulser/plate mesh point locations ($\alpha = 1$, 29 m \times 4 m plate, 8 m or 2 m slats, DX = 1)	40

ILLUSTRATIONS (Continued)

<u>Figure</u>		<u>Page</u>
19	Pulser I, Z and plate I for source end	41
20	Pulser I, Z and plate I for center location	42
21	Pulser I, Z and plate I for far end location	43
22	Slat/pulser/plate mesh point locations ($\alpha = 1$, 29 m \times 4 m plate, 9 pulsers, DX = 1)	44
23	Currents for source end observer 1, for cases $\alpha = 1$, 29 m \times 4 m plate, 8 m slats, DX = 1, 19 pulsers; $\alpha = 1$, 29 m \times 4 m plate, 8 m slats, DX = 1, 9 pulsers	45
24	Currents for midpoint observer 4, for cases $\alpha = 1$, 29 m \times 4 m plate, 8 m slats, DX = 1, 19 pulsers; $\alpha = 1$, 29 m \times 4 m plate, 8 m slats, DX = 1, 9 pulsers	46
25	Ground rods connected to end plates	47
26	Pulser and wire currents w/wo ground rods (OBS 1, near source)	48
27	Pulser and wire currents w/wo ground rods (OBS 4, center)	49
28	Pulser and wire currents w/wo ground rods (OBS 7, far end)	50
29	Buried wire connected to ground rods	51
30	Pulser and wire current for 29 m wire open and 54 m wire shorted to ground rods (OBS 1, near source)	52
31	Pulser and wire current for 29 m wire open and 54 m wire shorted to ground rods (OBS 4, center)	53
32	Pulser and wire current for 29 m wire open and 54 m wire shorted to ground rods (OBS 7, far end)	54
33	Coarse grid geometry for 4 m mesh	55
34	Source voltage for coarse mesh calculations	56

ILLUSTRATIONS (Concluded)

<u>Figure</u>		<u>Page</u>
35	Coarse mesh, 4 m Δ 's, wire currents (center)	57
36	Coarse mesh, 4 m Δ 's, wire currents, 8 m and 40 m long slats, center positioned wire and off center wire	58
37	Coarse mesh, 4 m Δ 's, wire currents, 40 m long slats, two ground conductivities (0.001 and 0.01)	59
38	Coarse mesh, 4 m Δ 's, wire currents, 40 m long slats, two ground conductivities (0.001 and 0.01)	60

I. INTRODUCTION

This note summarizes several specific calculations relating to the interaction between a DISCUS type simulator and buried conductors. The DISCUS simulator is a serially arranged number of pulsers positioned near the surface of the ground (e.g., Ref. 1). In operation, the pulsers are sequentially fired to simulate the passing EMP wave from a nuclear surface burst. Interacting objects in these calculations are positioned below the ground surface.

Initial "late-time" DISCUS calculations were made to 3 μ s using a uniform 4 m mesh in the A3D code (Ref. 2). Large time steps could be taken, but at the expense of accurately describing the fast rising source. More uncertainty must be attached to these results because of the coarse mesh. The remainder of the calculations were made using a uniform 1 m mesh. This provided a compromise between the coarse mesh late-time model requiring reasonable computer resources and a mesh less than 0.4 m useful for early time but requiring excessive computer resources to go beyond a few hundred nanoseconds. The 1 m mesh calculations cover from 0-720 ns. Interaction with two conductor types were considered-- a perfectly conducting wire (an antenna or cable) and a perfectly conducting plate (a missile shelter perhaps).

-
1. Baum, C. E., "A Distributed-Source Conducting Medium Simulator for Structures Near and Below the Ground Surface," EMP Sensor and Simulation Note 87, Air Force Weapons Laboratory, Kirtland AFB, NM, 9 July 1969.
 2. Marks, J. A., "A User's Manual for the Three-Dimensional A3D Electromagnetic Scattering Code," DC-TN-1222-14, Dikewood Industries, Inc.; November 1976 (also published as AFWL-TR-77-23).

Results show the relationship between the pulser currents, pulser impedances, and currents induced on the buried wire or plate as a function of position along the DISCUS array. Electric fields normal to the wire are given for some cases.

Computations are performed numerically using a double exponential (over/under) source and a finite difference time domain Maxwell solver, A3D. Typical mesh dimensions are shown in Figure 1.

Section IV.1 gives results for the 37 m and 29 m long wires buried under a 19 pulser array. In addition to the pulser current, pulser impedance, and wire current, the electric fields normal to the wire are given as a function of position along the wire.

Section IV.2 describes problems encountered with defining a faster source ($\alpha = 2$) in the 1 m mesh. The results are more ragged but illustrate the same general response characteristics at the slower ($\alpha = 1$) source.

Section IV.3 shows the effect of varying the pulser slat length between 2 m and 8 m and the corresponding currents induced on a 4 m wide plate buried 1 m.

Section IV.4 shows the variation in the pulser and buried plate current when a 9 pulser array replaces the normal 19 pulser array. This was modeled by replacing every other pulser location with an additional conducting plate which filled the gap between the original plates. The voltages of the remaining pulsers were increased by the ratio of 19/9.

Section IV.5 shows the effect of positioning ground rods at the ends of the pulser array and actually shorting these rods to the end plates of the DISCUS array. The buried wire remains shorter overall than the array.

Section IV.6 shows the effect of positioning the ground rods outside of the pulser array and then lengthening the buried wire and connecting it to the ground rods.

Section IV.7 gives results from the coarse mesh calculations. These calculations indicate late time results to 3 μ s.

II. GEOMETRY AND MESH

The majority of these calculations were based on a uniform 1 m mesh in the A3D code. Table 1 gives meshing coordinates and Figure 1 depicts the overall dimensions. Slight differences in geometry are noted with each separate calculation.

TABLE 1. GEOMETRY AND MESH COORDINATES

Mesh Sizes

DX = 1, no. cells = 51; total X = 50 m
DY = 1, no. cells = 30; total Y = 29 m
(symmetry plane)
DZ = 1, no. cells = 60; total Z = 59 m

X Components

Cable from 12-40 (mesh point locations)
Total Length = 29 m
20 plates (from 6 m to 44 m)

Y Components

Symmetry
Center of rods (or plates) at $Y = 0$
Rod (or plates) length
2 m long (1 mesh + symmetry)
8 m long (4 meshes + symmetry)

Z Components

Air/ground at mesh point 31
Total ground depth = 30 m
Total air above ground = 29 m
Cable located 1 m below interface

Physical Constants

Dielectric constant of ground = $10 \epsilon_0$
Ground conductivity, $\sigma_g = 0.001$ S/m
(some cases with $\sigma_g = 0.01$ S/m)

III. SOURCE DESCRIPTION

Sources used for the 1 m mesh calculations are defined by an over/under exponential of the form

$$V(\tau) = \frac{A_o e^{\alpha\tau}}{1 + e^{2(\tau-\tau_p)}}$$

α was set to 10^8 or 2×10^8 /s and referred to as $\alpha = 1$ or $\alpha = 2$. Figure 2 shows difference in rate of rise. $\alpha = 1$ rises 10 to 90% in 25 ns, $\alpha = 2$ rises in 15 ns.

To simulate the surface burst conditions and the DISCUS simulator itself, the electric field at the mesh point between two slats (plates) is set each time step using the double exponential to determine the magnitude. These source mesh points are defined in Figure 3a. Setting only the center-most E_x is referred to as "center fire," while "all fire" is defined as setting the E_x field at all mesh positions to the end of the plate. Each source point is separated by $2\Delta X$ or 2 m for these cases. Four-hundred time steps of 1.8×10^{-9} s for a total time of 0.72 μ s were used. Each source mesh point relative time is retarded by $2\Delta X/C$ to simulate the surface burst source wave passing over the array at the speed of light.

IV. RESULTS

Tables 2 and 3 list the principal parameters varied for the DISCUS results to follow. Specific differences between cases are described under each subsection.

TABLE 2. PARAMETERS USED IN THE 1 m MESH CALCULATIONS

Run No.	Source α^a	Wire/Plate Dimensions			DX (m)	No. Pulsers	Slat Length (m)	Ground Rods Y/N
		Length (m)	Width (m)					
495	1	Wire	37	-	1	19	8	N
496	2	Wire	29	-	1	19	8	N
497	1	Plate	29	4	1	19	8	N
498	1	Plate	29	4	1	19	2	N
499	1	Plate	29	4	1	9	8	N
500	1	Wire	29	-	1	19	8	N
504	1	Wire	29	-	1	19	8	Y
505	1	Wire	54	-	1	19	8	Y

^aRise rate is given in units of inverse shakes (1 shake = 10 ns).

TABLE 3. PARAMETERS USED IN THE 4 m MESH CALCULATIONS

Run No.	Wire Location	Source Definition ^a	Slat Length (m)	σ_g (S/m)
467	Center	AF	40	0.01
468	Center	AF	40	0.001
469	Center	CF	40	0.01
470	Center	CF	40	0.001
471	Center	CF	8	0.001
472	Off center	CF	8	0.001
474	Off center	CF	40	0.001
475	Center	Environment	-	0.001
476	Center	AF	8	0.001

^aAF for "all fire," E_x set all meshes along slats.

CF for "center fire," E_x set at center mesh point only.

1. CASE 1: $\alpha = 1$, 37 m WIRE, 8 m SLATS, DX = 1, 19 PULSERS

Stylized mesh point and observer numbering are depicted in Figure 4. Results given in Figure 5 show the peak pulser current and peak wire current along the simulation length. Pulser and wire currents are largest at the midpoint of the length of wire. The 37 m wire is overlapped at the ends by the slat structure. Slats are 8 m long. Time domain results for three axial positions are given in Figures 6-8. Each figure depicts the pulser current, pulser impedance, and wire current for pulser numbers 2, 10, and 18. There are 19 pulsers altogether. Pulser number 10 is at the center. Pulser number 1 is at the source end of the mesh.

$\alpha = 1$, 29 m WIRE, 8 m SLATS, DX = 1, 19 PULSERS

Electric fields normal to wire--This calculation differs from the previous example by using a wire only 29 m long rather than the 37 m length (see Fig. 9). Two electric field components are used to estimate voltages at or near the wire, E_y , the horizontal component, and E_z , the vertical component. Figure 10a shows the maximum electric field observed at each observer position along the wire and Figure 10b shows the late time ($\sim 0.7 \mu\text{s}$) electric fields along the wire. In both cases, the maximum fields occur near the midpoint of the wire along with the largest currents. Figures 11-13 show time domain currents and E-fields for near, center, and far locations along the 29 m wire.

2. CASE 2: $\alpha = 2$, 29 m WIRE, 8 m SLATS, DX = 1, 19 PULSERS

An $\alpha = 2$ source in the 1 m mesh produces more oscillations in the observed currents (due to the mesh cell size) than the $\alpha = 1$ source but only slightly less overall current than the $\alpha = 1$ source. Pulser and wire current maximums along the length of the DISCUS are given in Figure 14. Pulser current, load impedance, and corresponding wire current (i.e., directly below) are given for near, center, and far locations in Figures 15-17.

3. COMPARISON 1: 2 m VS. 8 m LONG SLATS

$\alpha = 1$, 29 m \times 4 m plate, 8 m slats, DX = 1, 19 pulsers
 $\alpha = 1$, 29 m \times 4 m plate, 2 m slats, DX = 1, 19 pulsers

For this comparison, a buried, thin, rectangular conducting plate replaces the buried wire. Pulser currents and plate currents are compared when the slat lengths are either 8 m or 2 m. The source time history is the $\alpha = 1$ designation and the pulsers continue to operate in the "center fire" mode.

The buried plate, 29 m \times 4 m, is situated 1 m below the air/ground interface, the same as for the wire cases. The 19 pulser array is used. Figure 18 depicts the mesh point locations in the longitudinal direction for pulser, plates, and observers. The pulser array continues to overlap the plate by 5 m on each end.

In this comparison set, the 8 m slats overlap the buried plate, while in the 2 m long slat case, the slats do not cover the plate but are 1 m short on each side.

Figures 19-21 depict the pulser current, pulser impedance, and plate surface current for three positions along the array. Observers 1, 4, and 7 are located as seen in Figure 18.

We can note the following from these comparisons. The early time rise portion of the induced plate current is unaffected by the change in slat length as is expected. This result was shown in the wire comparisons previously described. As time progresses, the longer slat lengths require more current to maintain the imposed pulser voltage. Corresponding increases occur in the plate surface current. In Figures 19-21, we see only a twofold decrease in currents when going from 8 m to 2 m slats. An inverse relationship holds for the pulser impedance.

4. COMPARISON 2: 9 PULSERS VS. 19 PULSERS

$\alpha = 1$, 29 m \times 4 m plate, 8 m slats, DX = 1, 19 pulsers
 $\alpha = 1$, 29 m \times 4 m plate, 8 m slats, DX = 1, 9 pulsers

In this comparison, the simulator geometry is altered such that only nine pulsers are fired and additional perfectly conducting slats are used to fill in the space between every other pair of slats. This, in effect, makes the slats 3 m \times 8 m. The stylized mesh point locations are given in Figure 22. To compensate for the "missing" pulsers and to maintain the same overall source, the voltage impressed between the slats at the nine pulsers is increased in the ratio of 19/9.

Comparisons of these two cases are given in Figures 23 and 24 for observer number 1, an end observer, and number 4, a mid-point observer. Results are similar in shape to currents calculated in the buried wire case, as expected.

Early time results show an increase in the pulser and plate current for the nine pulser array due to the increased local voltage source. In the nine pulser array, observer number 1 is

vertical rods are 54 m apart. The " $\alpha = 1$ " source is used with pulsers in the "center fire" mode. Ground conductivity = 0.001 S/m.

Figures 30-32 compare the pulser and wire currents for observers 1, 4, and 7 corresponding to near, center, and far ends of the 29 m wire. Only slight increases are seen in the pulser currents, while significant differences are noted in the wire current. Wire current at the center of the wire is significantly larger in the lengthened wire case and at the last calculated time, 720 ns, is almost a factor of 2 larger than the 29 m case. Currents are almost three times higher at observers nearer the ends.

7. COARSE MESH DISCUS CALCULATIONS TO 3 μ s FOR A BURIED UNINSULATED WIRE

Several coarse mesh DISCUS calculations were made using a uniform 4 m space mesh to look at buried bare wire currents to times to 3 μ s (Fig. 33). Clearly, mesh cells of this size are too large to resolve a fast rising source, but larger time steps can be taken so that a late time calculation can be made in a reasonable amount of computer time. In this calculation, the DISCUS is buried in a ground with dielectric constant = $10 \epsilon_0$ so that there is no air/ground interface. Table 4 gives the mesh parameters for these runs. Figure 34 shows the electric field used to drive the voltage between the rods. This source decreases to 9.35×10^3 V/m at 2.4×10^{-6} s and was held constant after that. Currents shown for these coarse mesh cases were observed at the center of the buried wire.

TABLE 4. PARAMETERS FOR 4 m MESH CASES

Mesh Sizes

$\Delta X = 4$ m; 51 steps for 200 m length

$\Delta Y = 4$ m; 30 steps for 116 m width

$\Delta Z = 4$ m; 60 steps for 236 m height*

X Components

Wire length = 52 m

Y Components

Symmetry at $Y = 0$

Center of slats** at $Y = 0$

Z Components

Source and pulser slats imposed at $Z = 31$

Wire located 1 mesh, i.e., 4 m below pulser slats

Dielectric constant = 10

* 120 m below pulsers, 116 m above pulsers..

** Slats are wires of 0.04 m diameter using a thin wire model in the 4 m mesh. Slat lengths of 8 m and 40 m used 1 mesh point for 8 m wire using symmetry plane, 5 mesh points for 400 m wire using symmetry plane.

a. Slat length variations and environment effects--Figure 35 shows a comparison of the observed current for four cases using the following parameter variations:

- (1) 8 m long rods (slats), source is fired across center of rods only.
- (2) 8 m long rods (slats), center and end fire.
- (3) 40 m long rods (slats), center fire and every 4 m along rods.
- (4) Environment.

The environment case is modeled by removing the rods (slats) and establishing the voltage source at all mesh points across the grid. Center firing across the short 8 m slats generates 60% of the current on the wire generated by the environment case.

b. Centered/off centered wire drive and slat length effects--Figure 36 shows the effect on the wire currents for different length rods (slats) when the center fire mode is used in both cases. Two wire positions are considered. In one case, the wire is positioned directly under the simulator and the other case has the wire positioned one mesh (4 m) to the side. Due to symmetry, this is equivalent to having two wires present. Observed current differences at early time due to changes in slat lengths are extremely small and at late times, $\sim 3 \mu\text{s}$, the differences are less than 10%. Slat length apparently has little to no effect, at least for those cases where the voltage source is established between the slats (or rods) as was done here.

c. Ground conductivity and pulser position effects--Figures 37 and 38 show results of varying the ambient conductivity between

0.01 and 0.001 S/m for 40 m long slats in the "center fire" and "fire all along" cases. The higher conductivity produces larger currents since maintaining the voltage source across the higher impedance ground conductivity requires more current. Interestingly, for the lower conductivity cases, the late time currents differ by only 20%, while the early time currents differ by closer to 30%. The late time currents are less dependent on the actual method of applying the source in the $\sigma_g = 0.001$ case, but this is not the case for the $\sigma_g = 0.01$ case where the ratio remains fairly constant throughout the time span. Figure 38 is Figure 37 redrawn with the $\sigma_g = 0.01$ cases normalized to the $\sigma_g = 0.001$ cases by reducing the currents by a factor of 10 to account for the differences in the source σE .

V. CONCLUSIONS

Several interesting conclusions can be drawn from this series of computer calculations. Modeling an EMP experiment with a finite difference code proves to be a highly efficient means of designing the experimental equipment required for system testing and evaluation.

1. The source rise rate, α , is only important if the system can respond to the faster rising currents induced along the buried conductor. Once the pulse has passed through the region the induced currents are not controlled by the rise rate.

2. A buried conductor initially responds to a single row of DISCUS pulsers to within a factor of two of the result seen for an infinite array of pulsers. The DISCUS pulser row can simulate the real environment within a factor of two if the source can be reproduced by the pulsers. After the pulse passes the agreement is within 25%.

3. Altering the slat length has little to no effect until the pulse peak has passed. Then the longer slat length increases the pulser current and conductor current proportionately. Short slats drive currents along the wire as well as long slats.

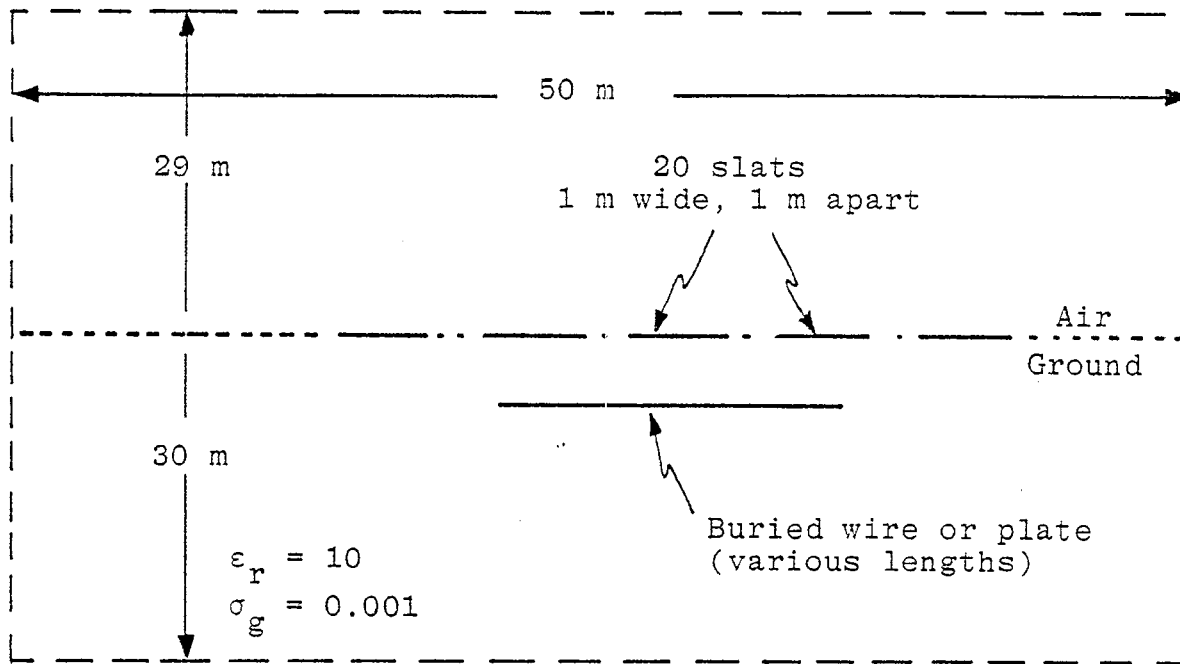
4. The DISCUS can be operated with fewer pulsers if the source voltage can be increased proportionately. Comparisons between 9 and 19 pulsers show good agreement for both early times near peak and at times approaching 1 μ s.

5. Ground rods added to the ends of the array have little effect on the early peak response. Significant increases in pulser current are required for the ground rod case, but only slight changes are noted in the induced buried conductor currents.

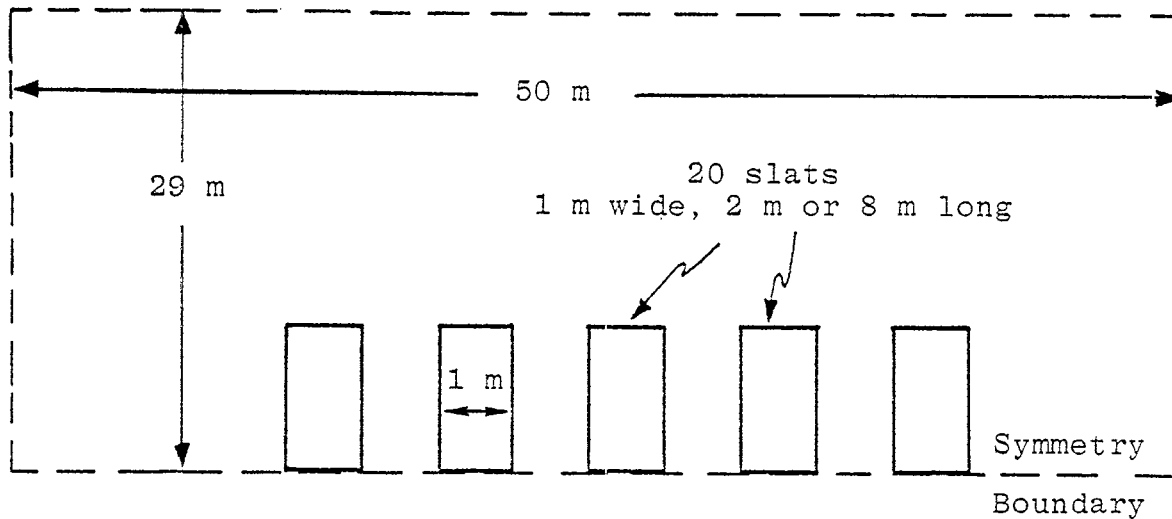
6. Different length buried wires respond the same initially until the pulse peak passes. Then the longer wire begins to carry significantly more current with little to no difference in the actual pulser current.

TABLE 5. SUMMARY OF BURIED CONDUCTOR RESPONSES
TO PARAMETER VARIATIONS

<u>Variable Parameter</u>	<u>Near Pulse Peak</u>	<u>Following Pulse Peak</u>
Source Rise Rate	Proportional	Not Significant
Pulser Row(s) (Environment)	Single Row Simulates Environment within Factor of 2	Single Row Simulates Environment within 30%
Slat Length	Not Significant	More Pulser Drawn More Conductor Current Seen
Number of Pulsers	Proportional	Less Important
With/Without Ground Rods	Not Significant	Significant Pulser Current Increase to Produce Same Conductor Current
Wire Length	Not Significant	Long Wire Picks Up More Current



Side View



Top View

Figure 1. DISCUS geometry with 1 m mesh.

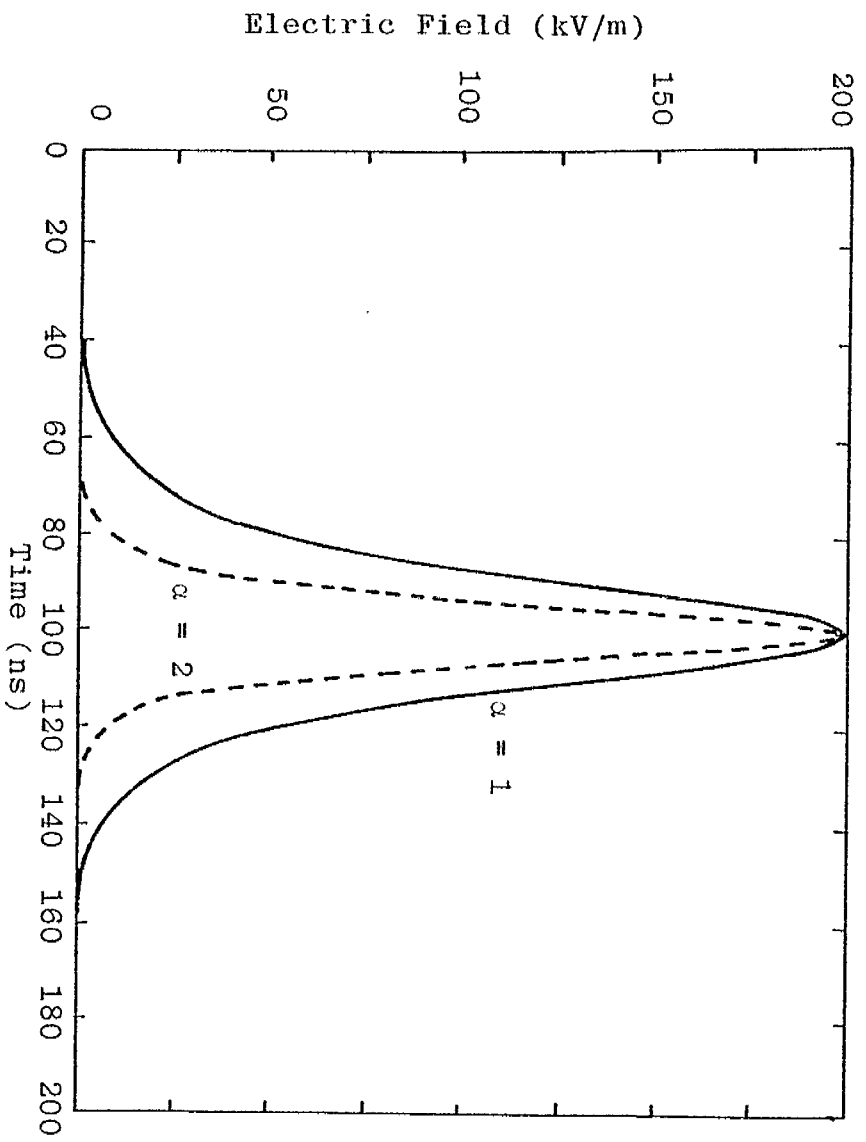


Figure 2. Source electric field.

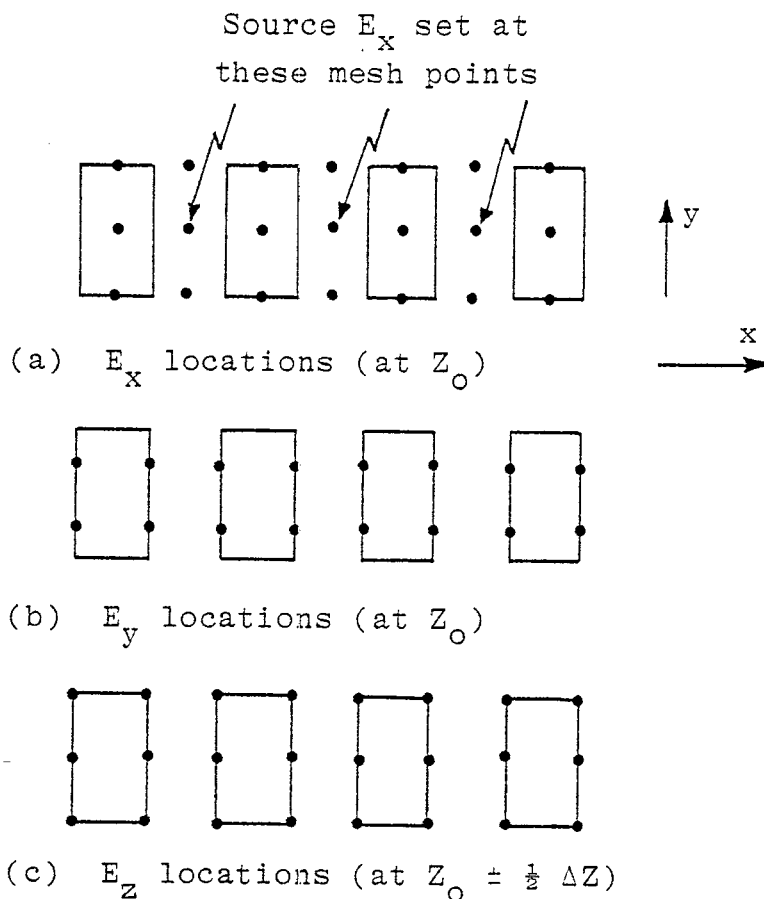


Figure 3. Top view (x,y) of E_x , E_y , and E_z mesh point locations for DX slats with slat length = 2 DY (slats are on Z_0 plane).

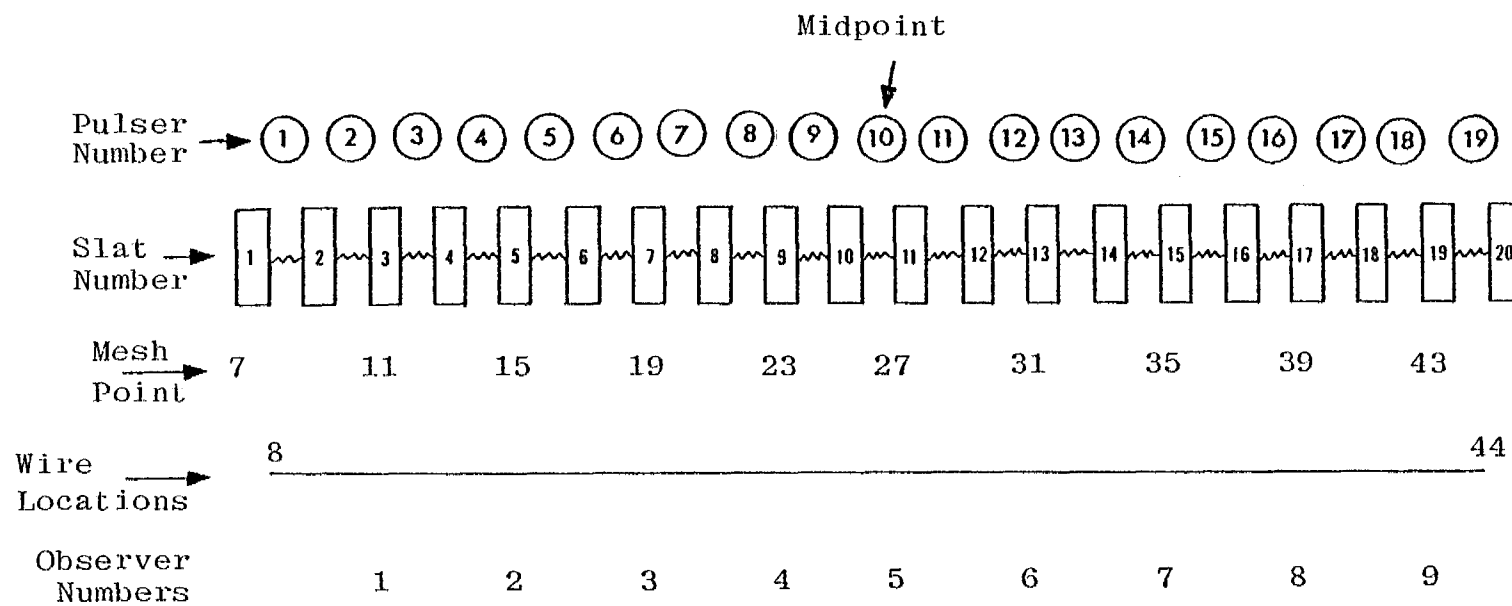


Figure 4. Slat/pulser/wire mesh point locations
(37 m wire, 8 m slats, $DX = 1$).

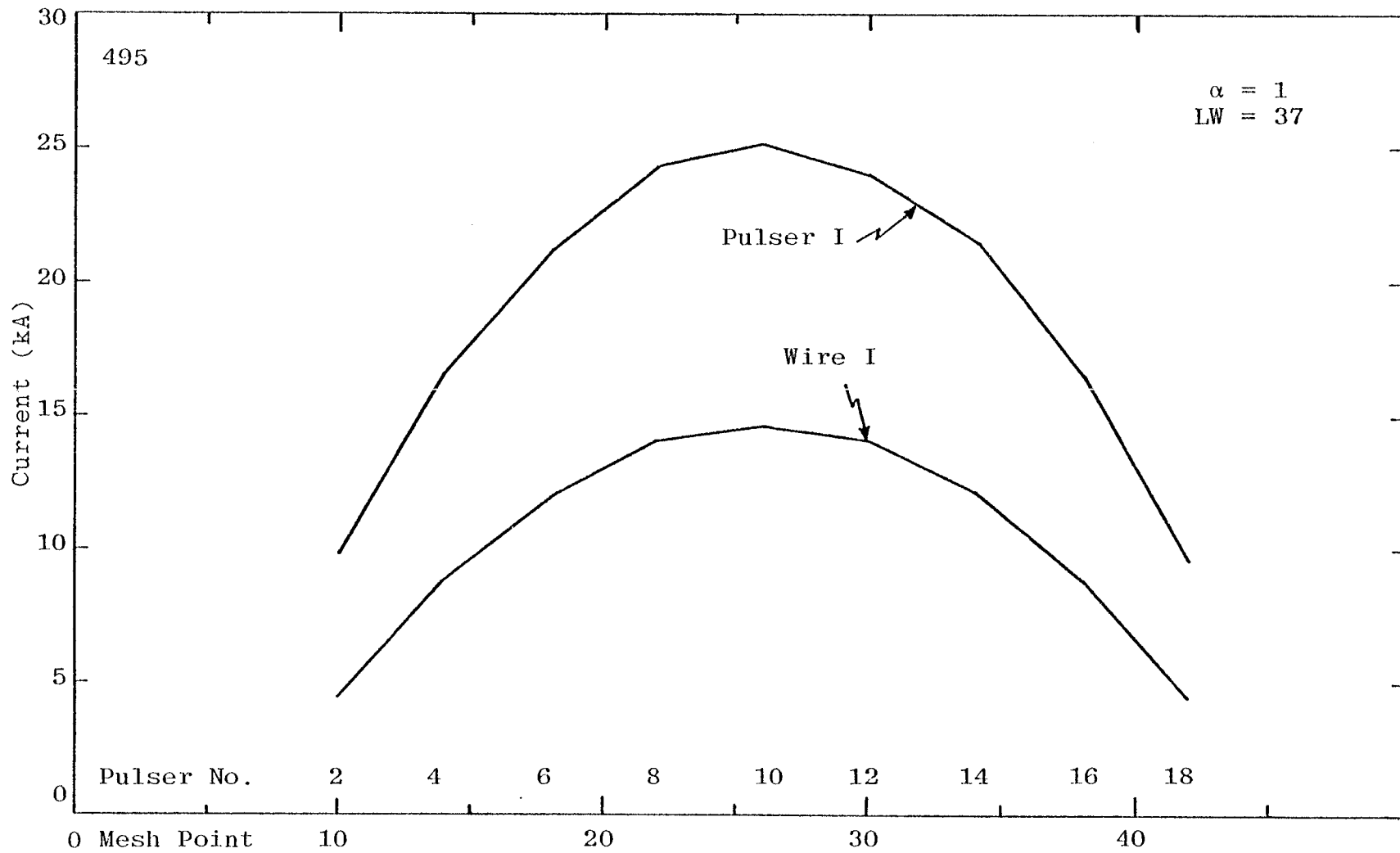


Figure 5. Pulser current and wire current along length of simulator.

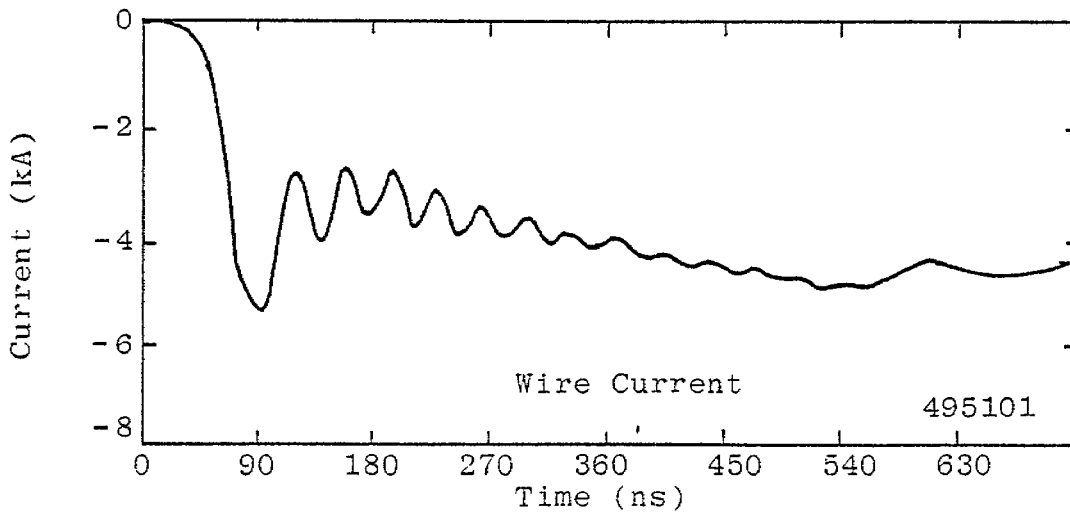
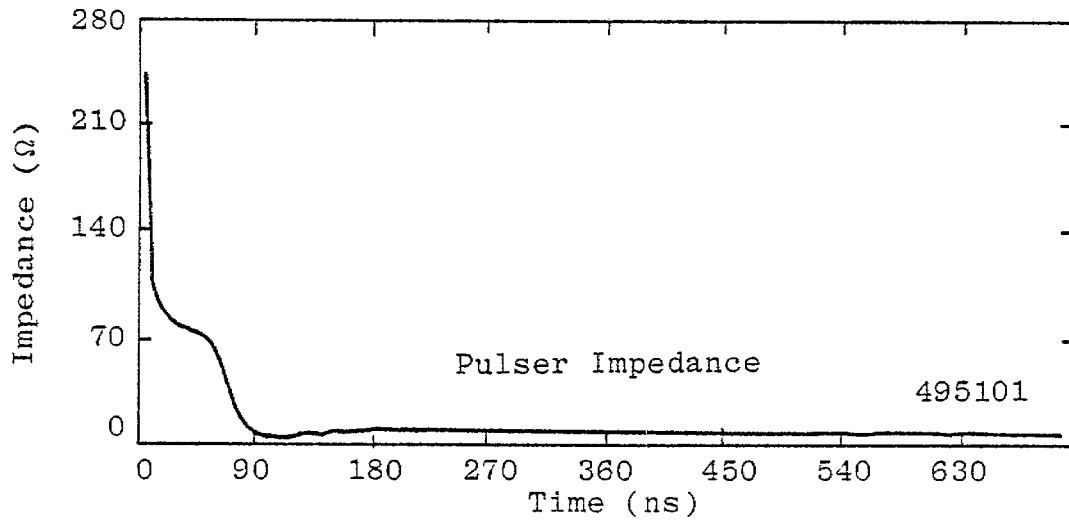
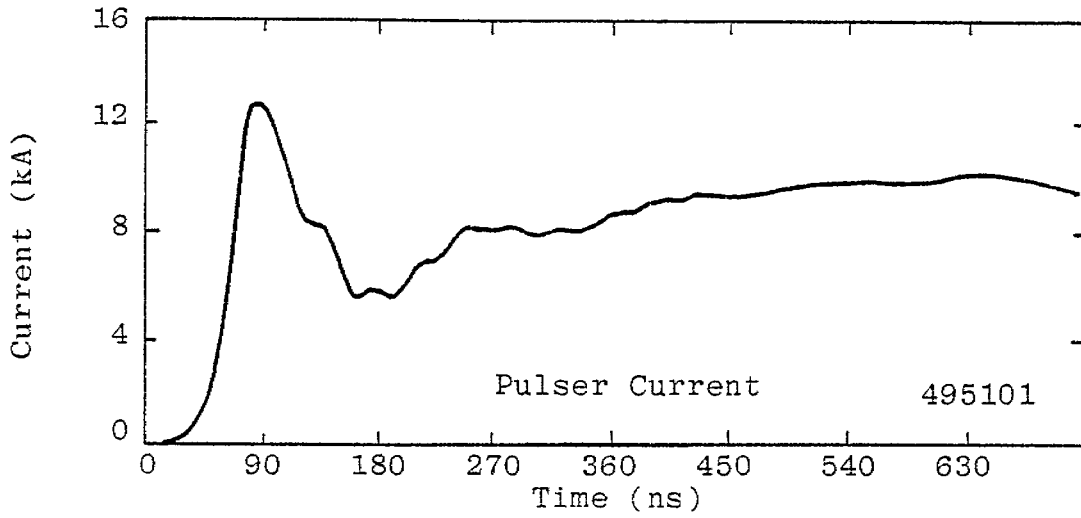


Figure 6. Currents at pulser no. 2 (source end, 9 m).

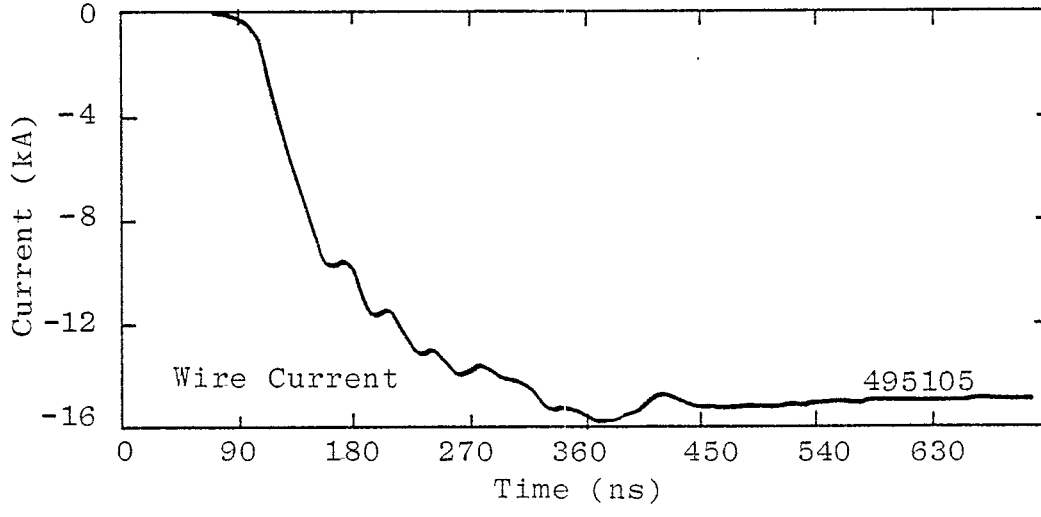
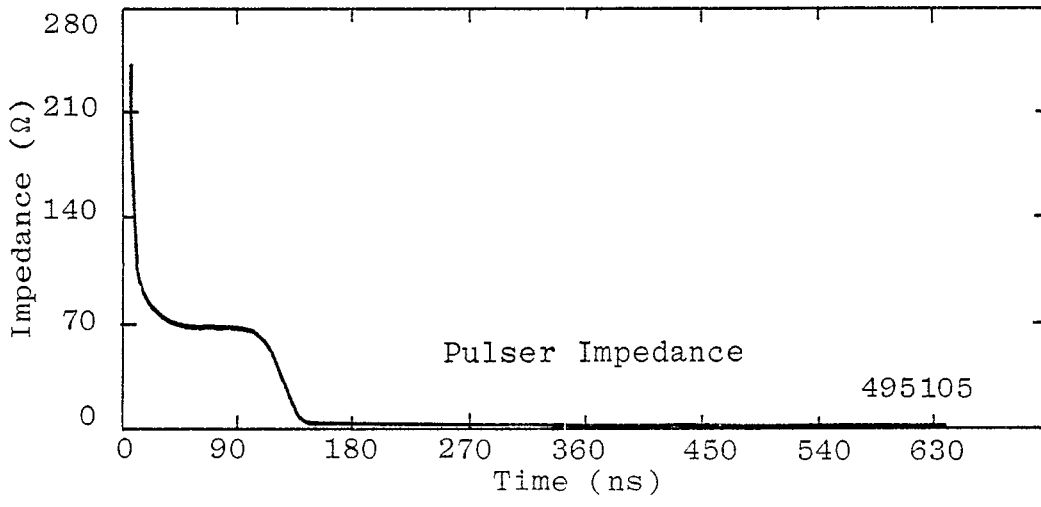
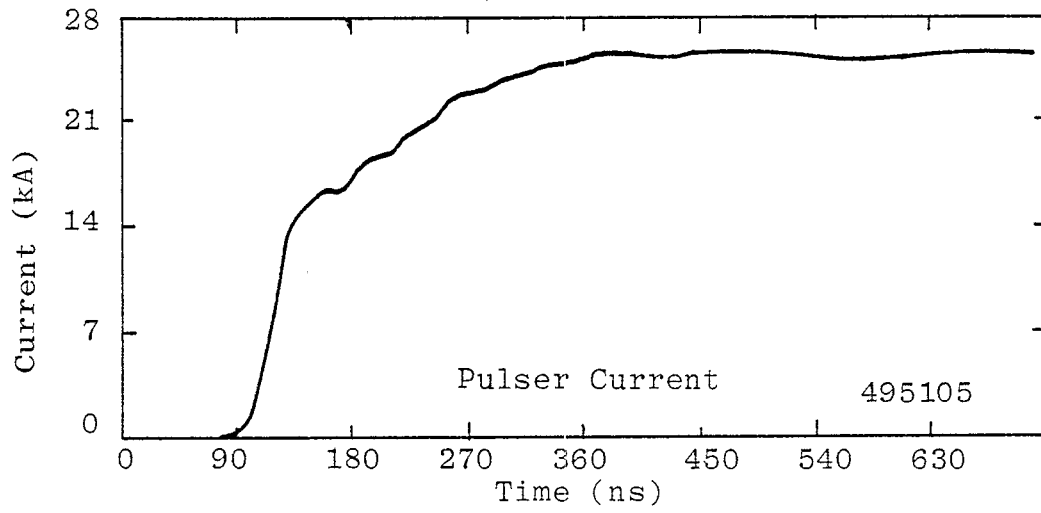


Figure 7. Currents at pulser no. 10 (center, 25 m).

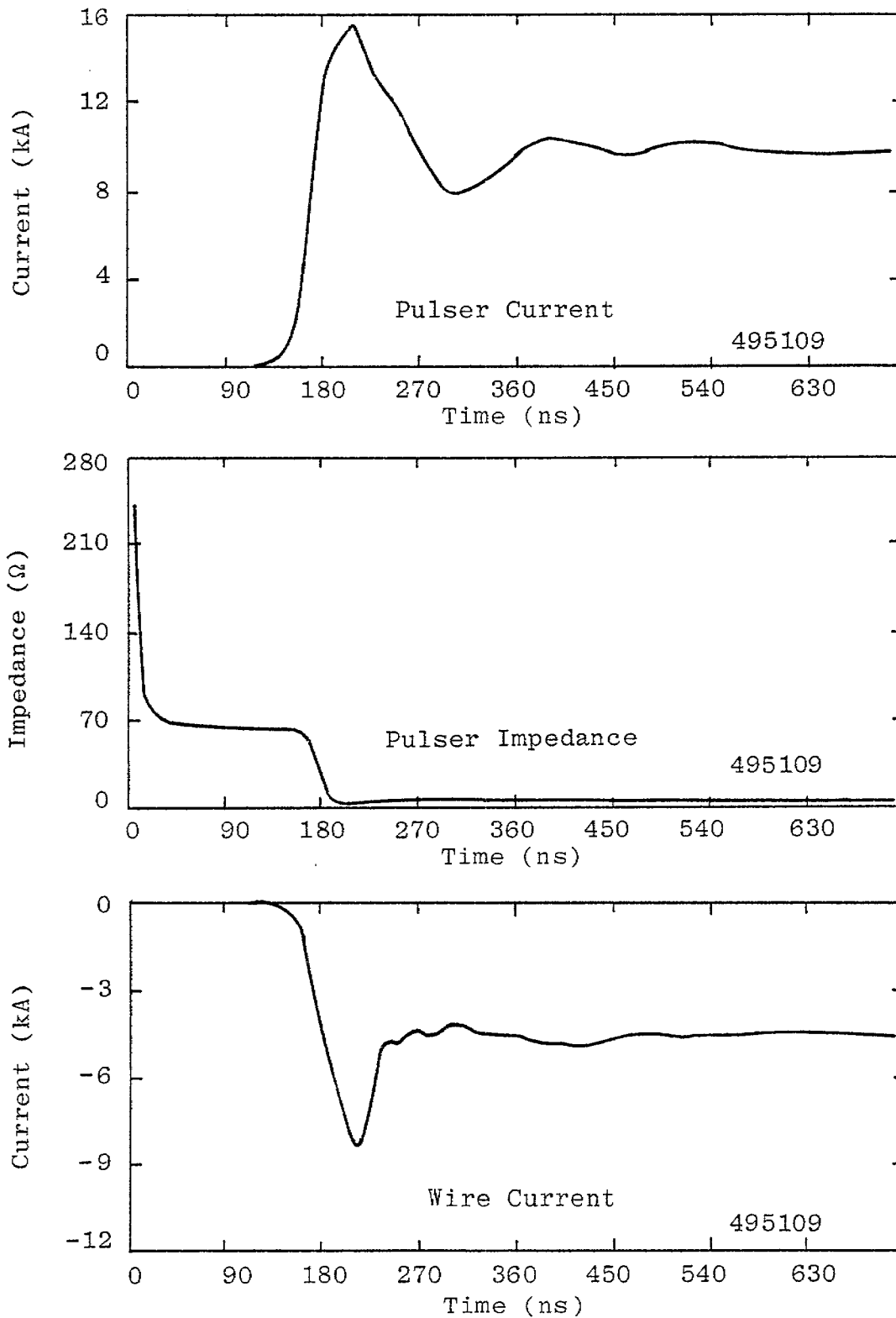


Figure 8. Currents at pulser no. 18 (far end, 41 m).

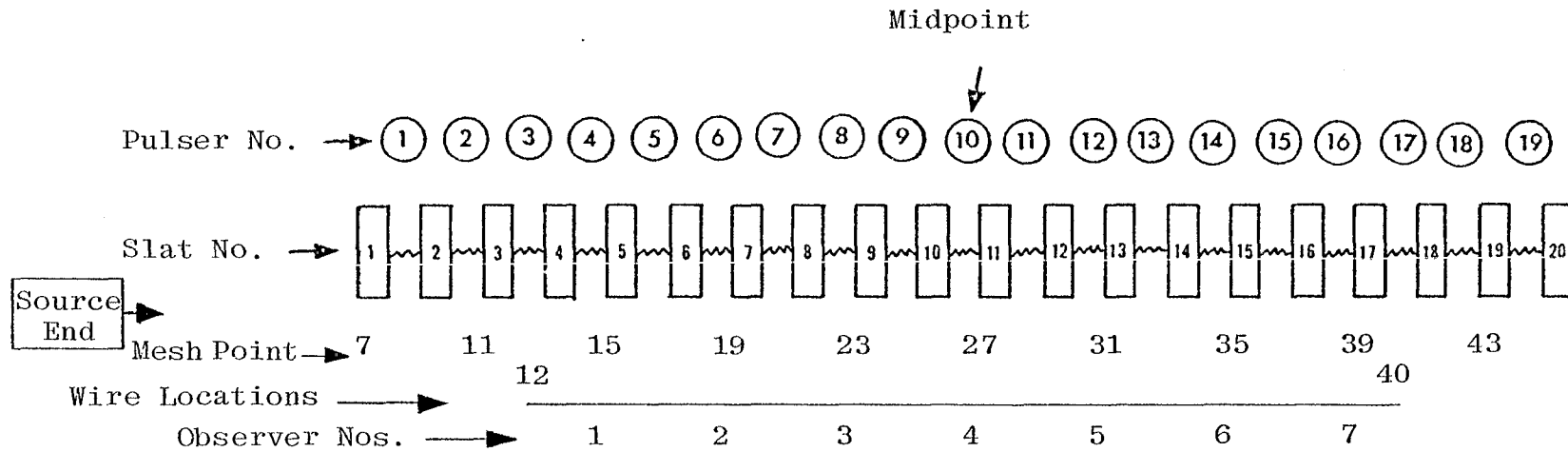
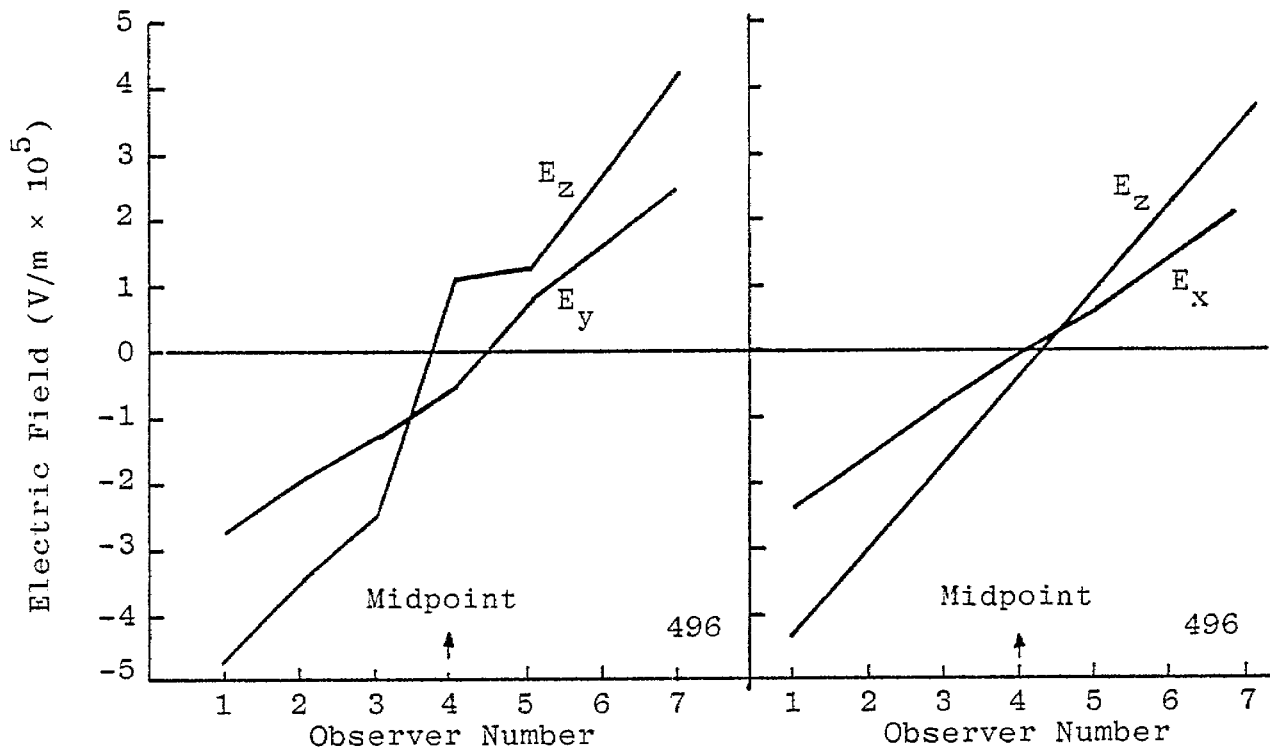


Figure 9. Slat/pulser/wire mesh point locations
(29 m wire, 8 m slats, $DX = 1$ m).



(a) Maximum electric field normal to wire, E_y (horizontal), E_z (vertical).

(b) Electric fields normal to wire at $t = 0.7 \mu\text{s}$.

Figure 10. Electric fields normal to 29 m wire.

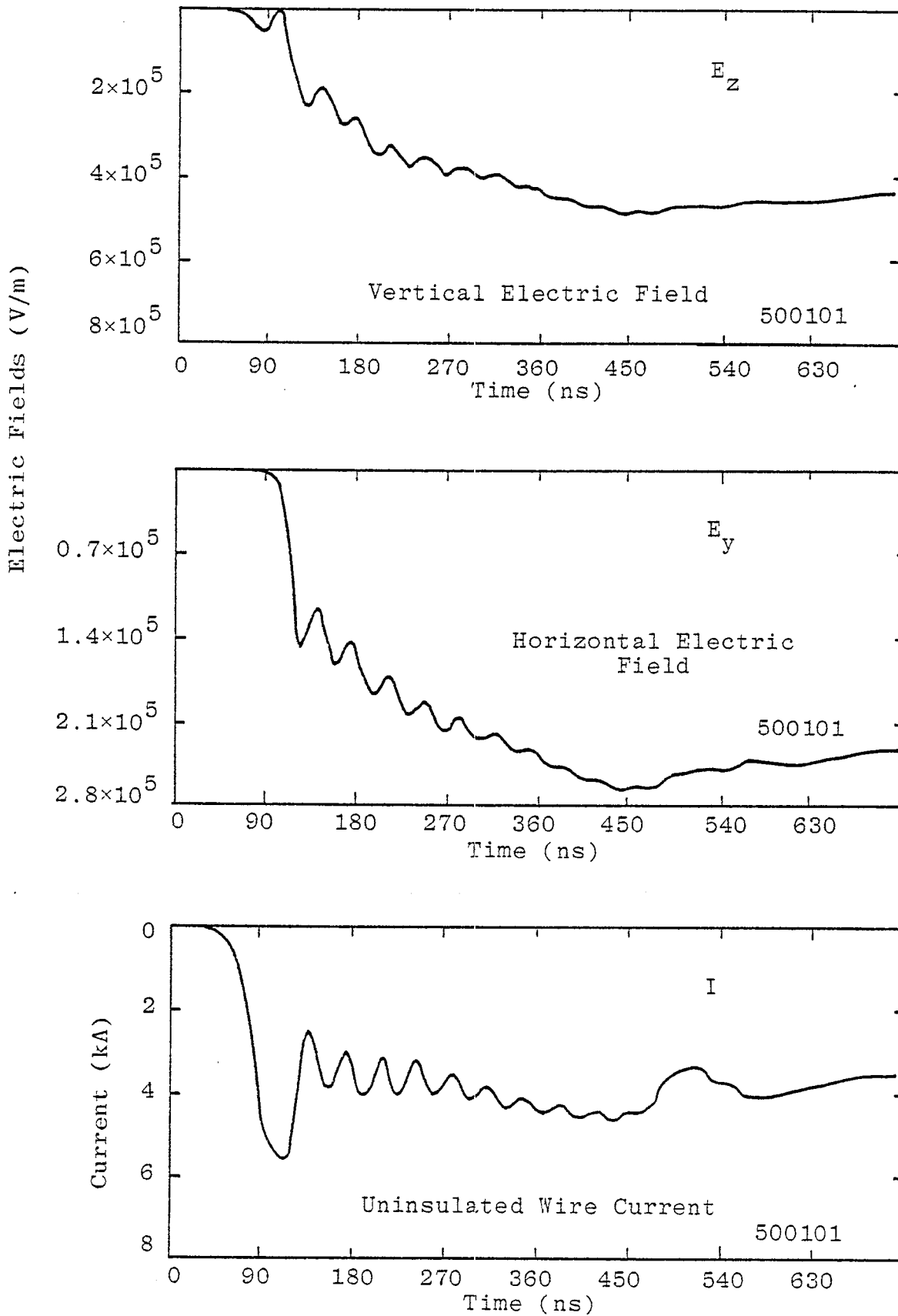


Figure 11. Wire current and normal electric fields 2 m from source end.

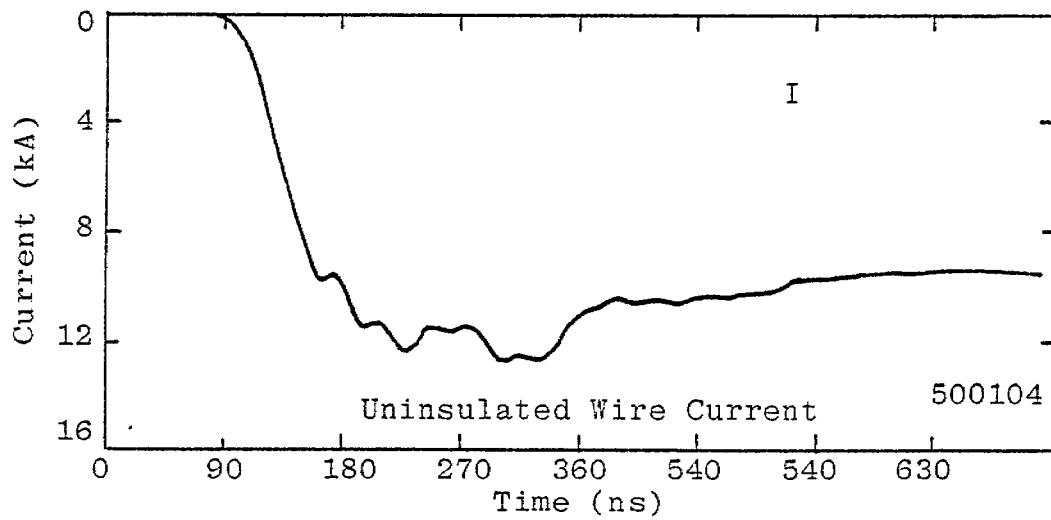
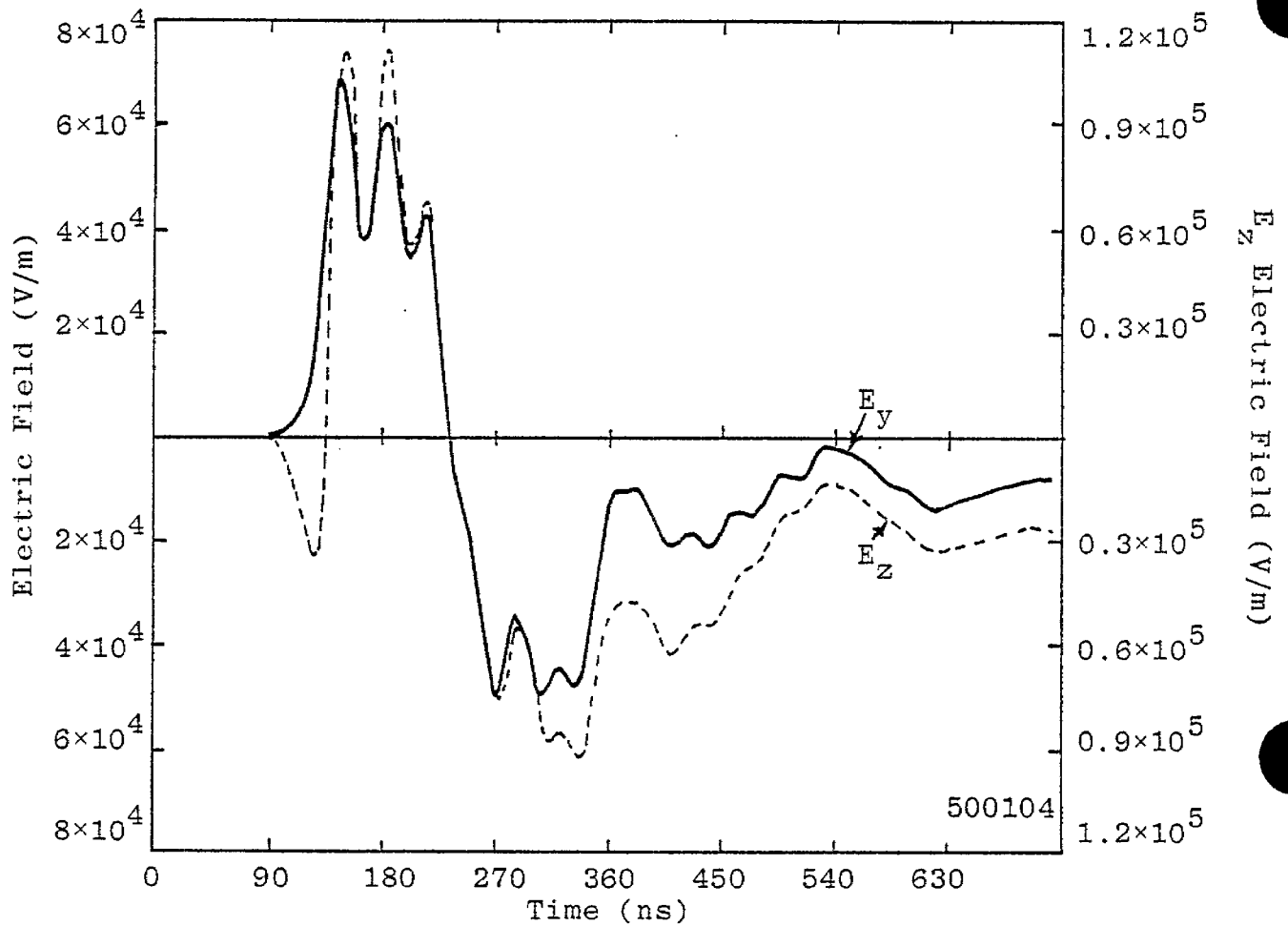


Figure 12. Wire current and normal electric fields at midpoint of 29 m wire.

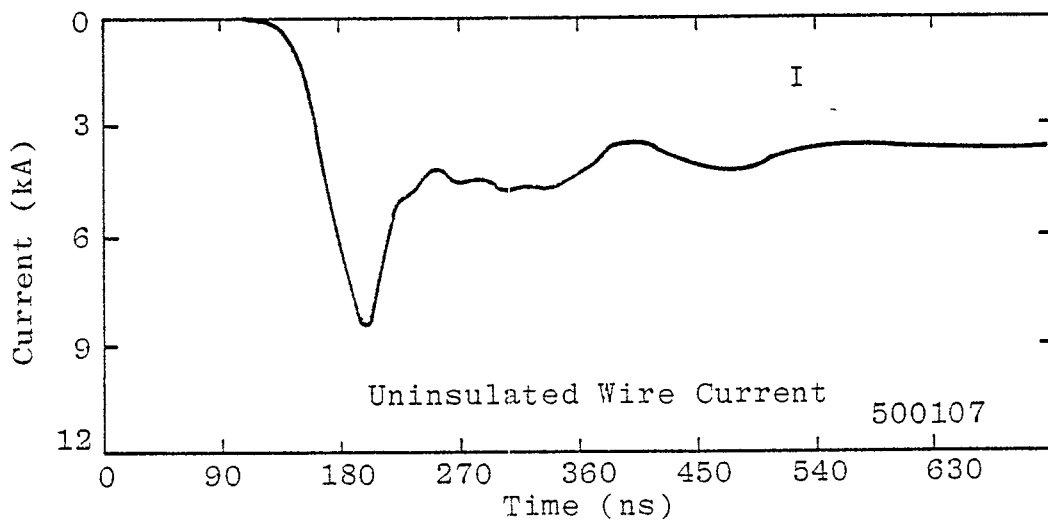
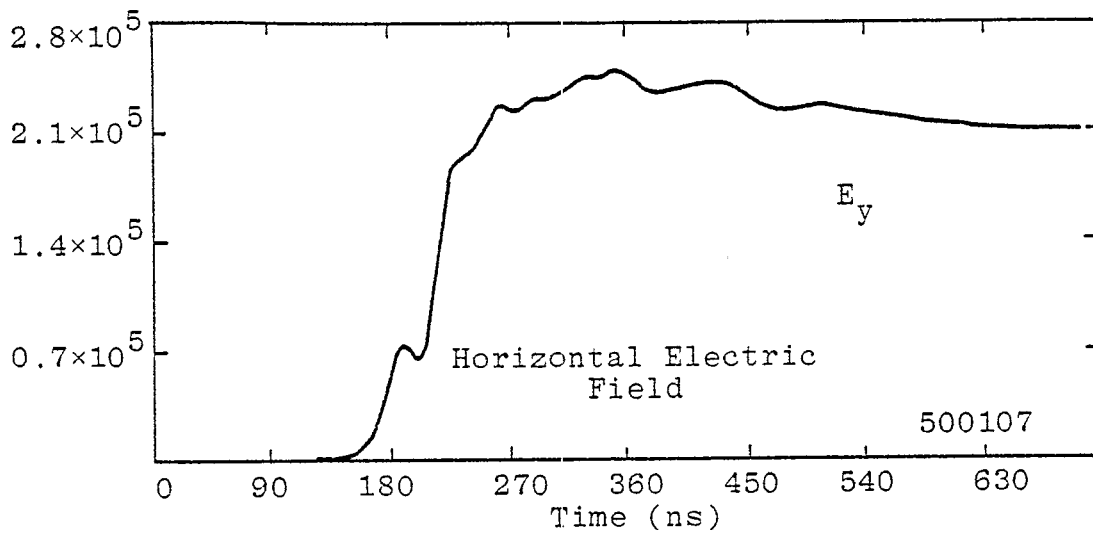
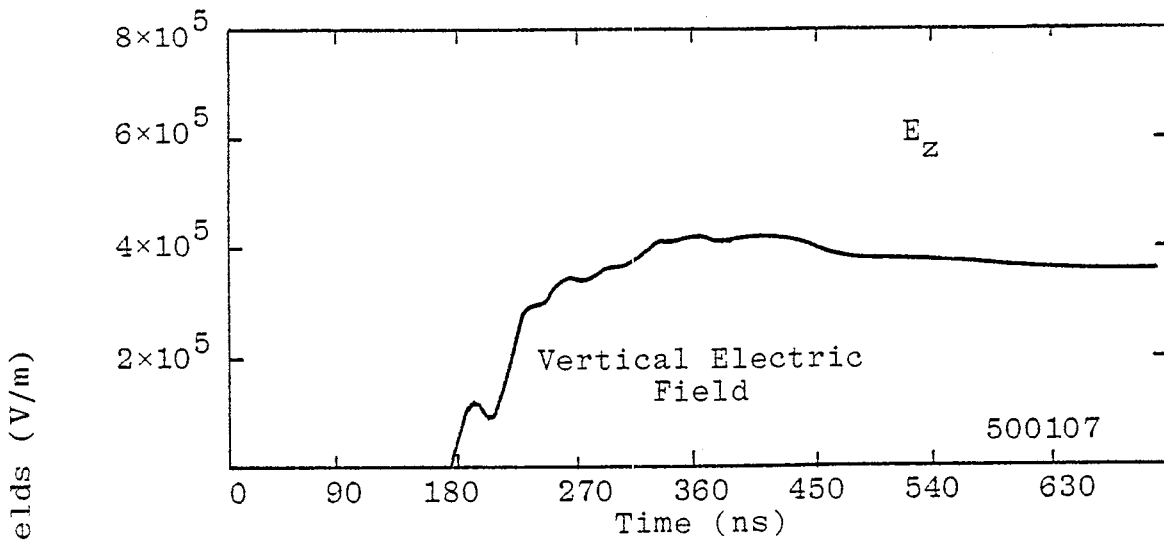


Figure 13. Wire current and normal electric fields 2 m from far end.

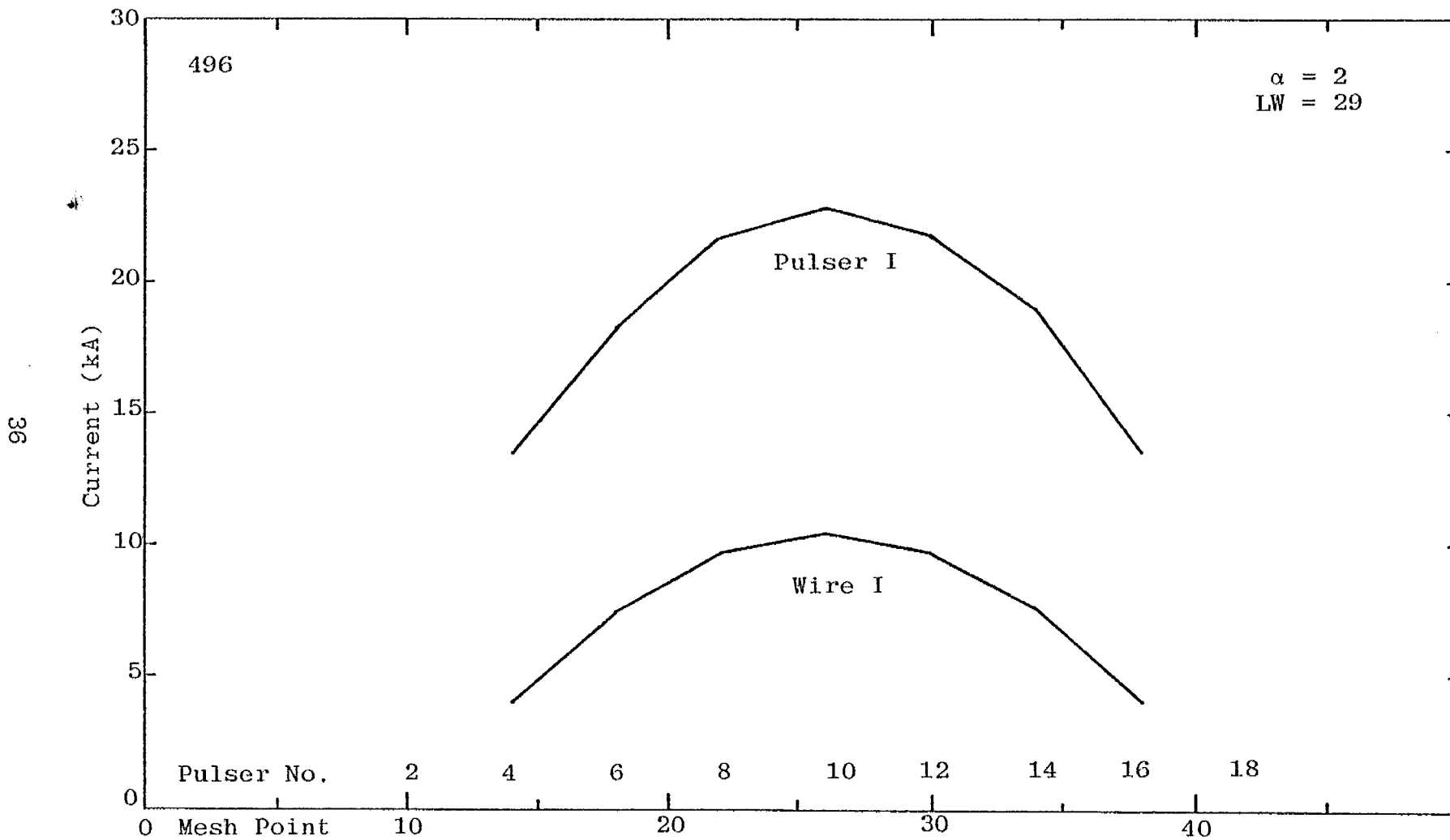


Figure 14. Pulser current and wire current along length of simulator.

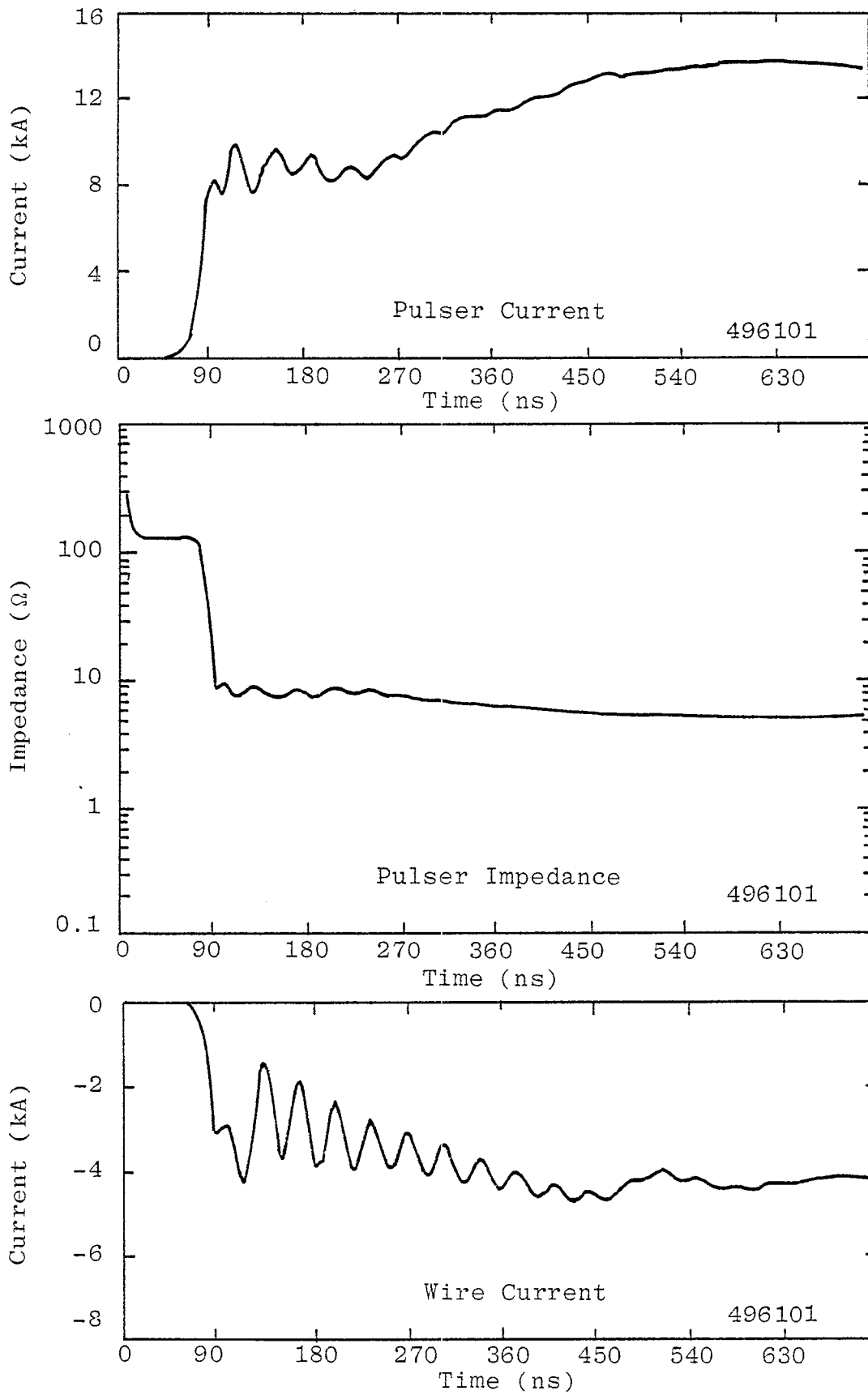


Figure 15. $\alpha = 2$, 29 m wire, 8 m slats, DX = 1, 19 pulsers, OBS-1.

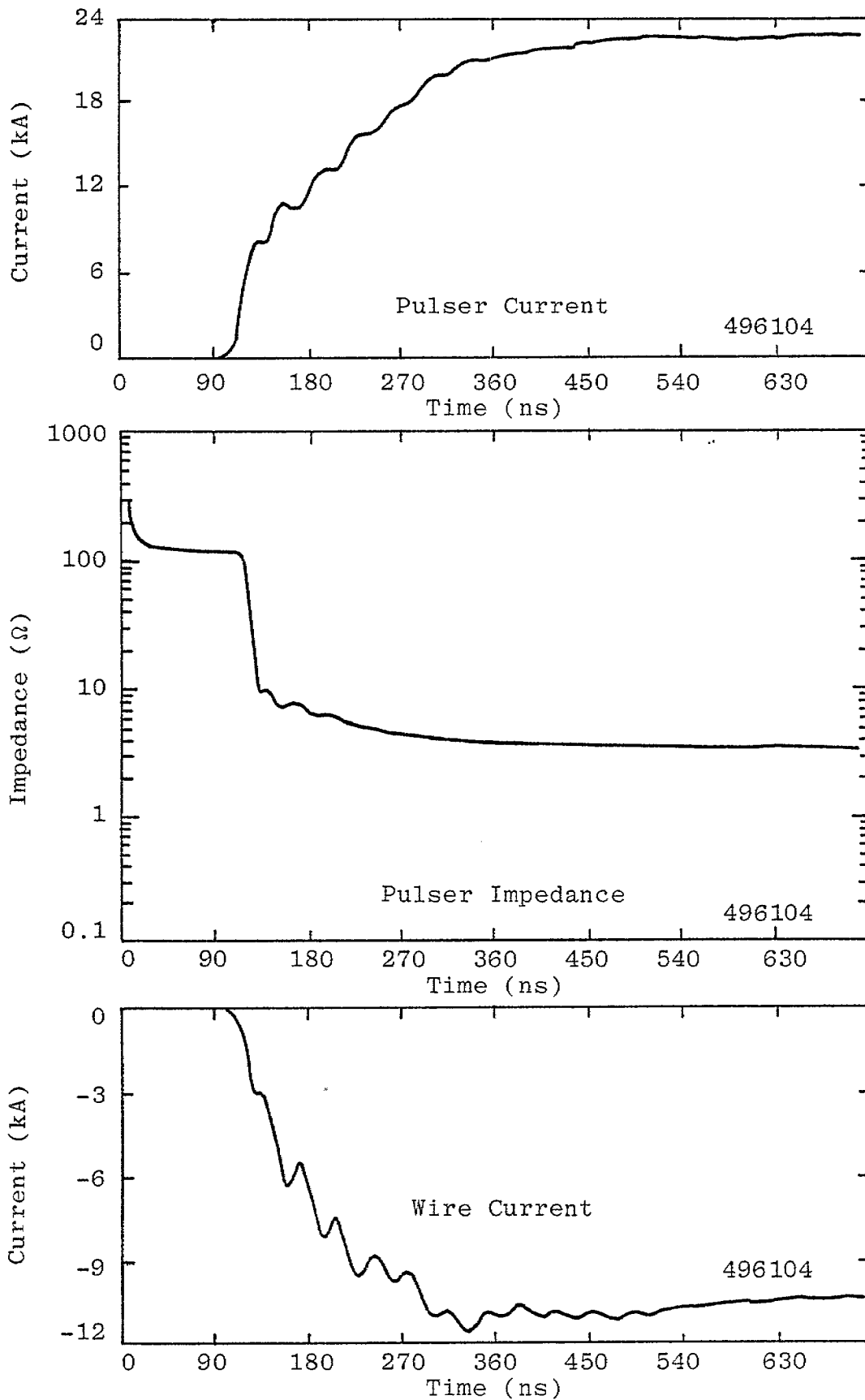


Figure 16. $\alpha = 2$, 29 m wire, 8 m slats, DX = 1, 19 pulsers, OBS-4 (midpoint).

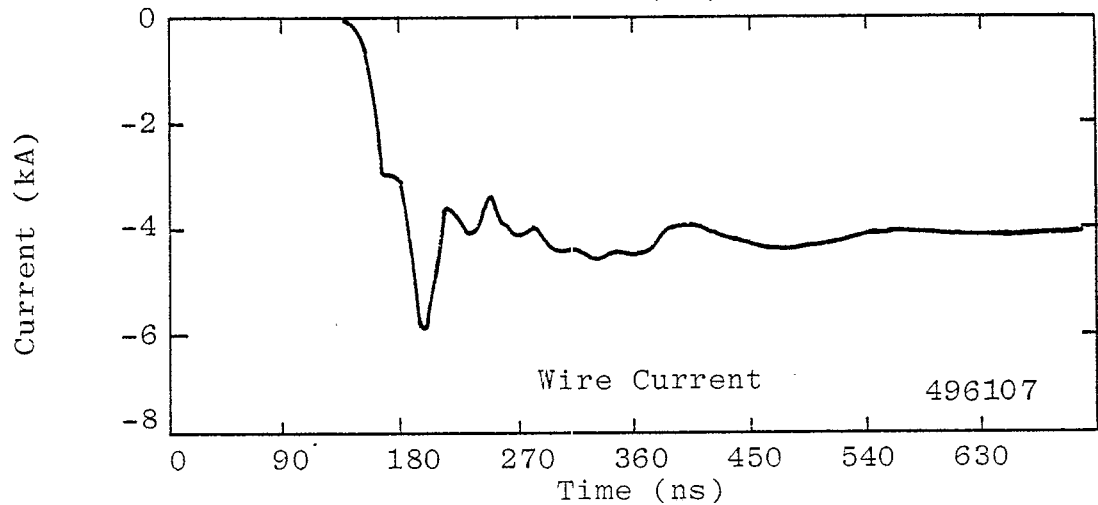
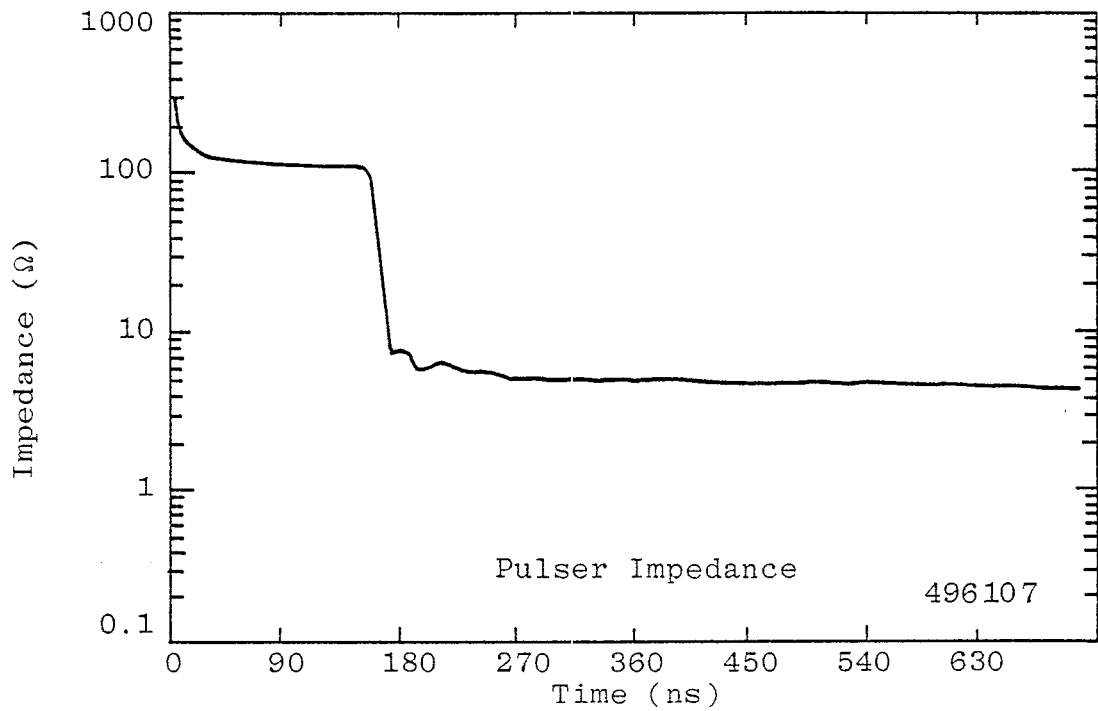
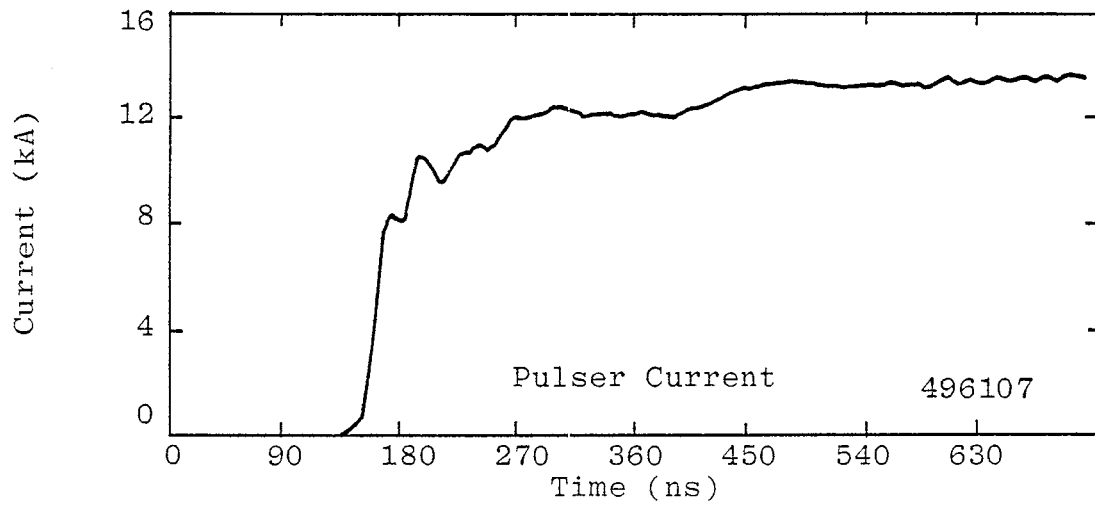


Figure 17. $\alpha = 2$, 29 m wire, 8 m slats, DX = 1, 19 pulsers, OBS-7

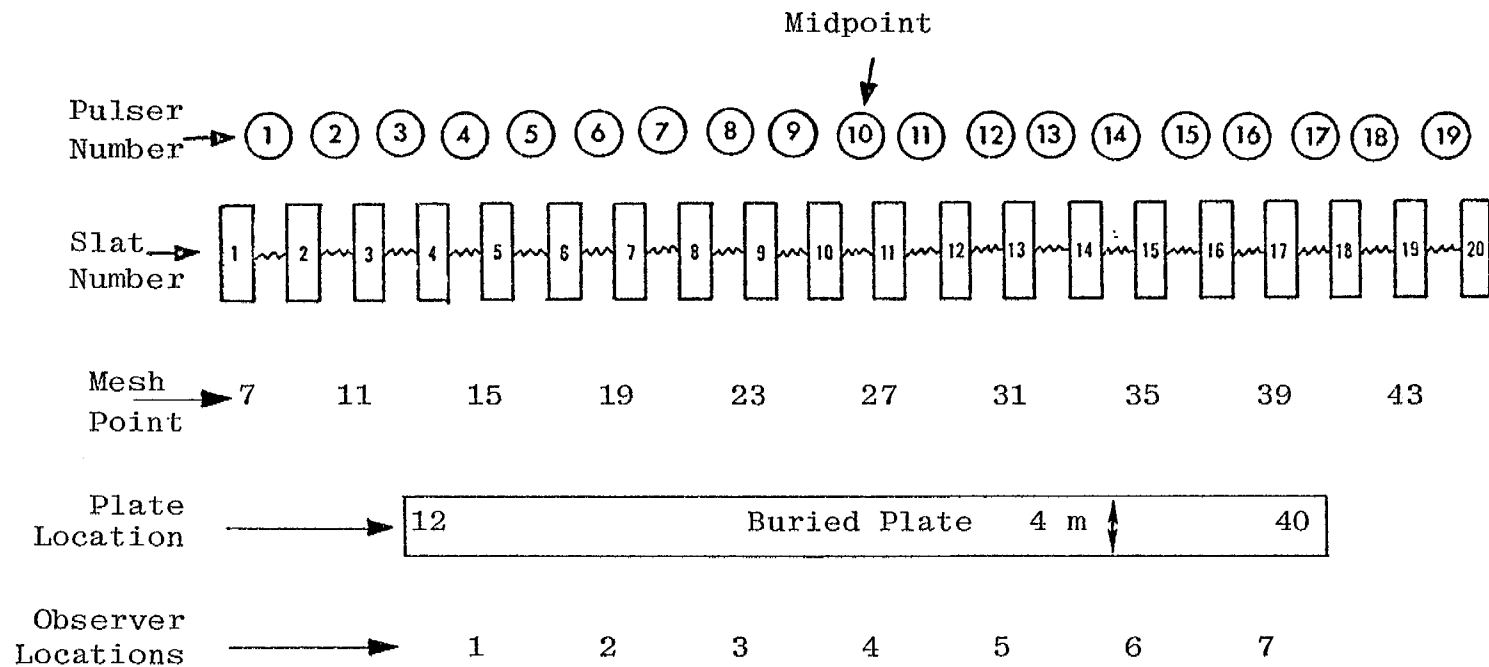


Figure 18. Slat/pulser/plate mesh point locations
 ($\alpha = 1$, $29 \text{ m} \times 4 \text{ m}$ plate, 8 m or 2 m slats,
 $DX = 1$).

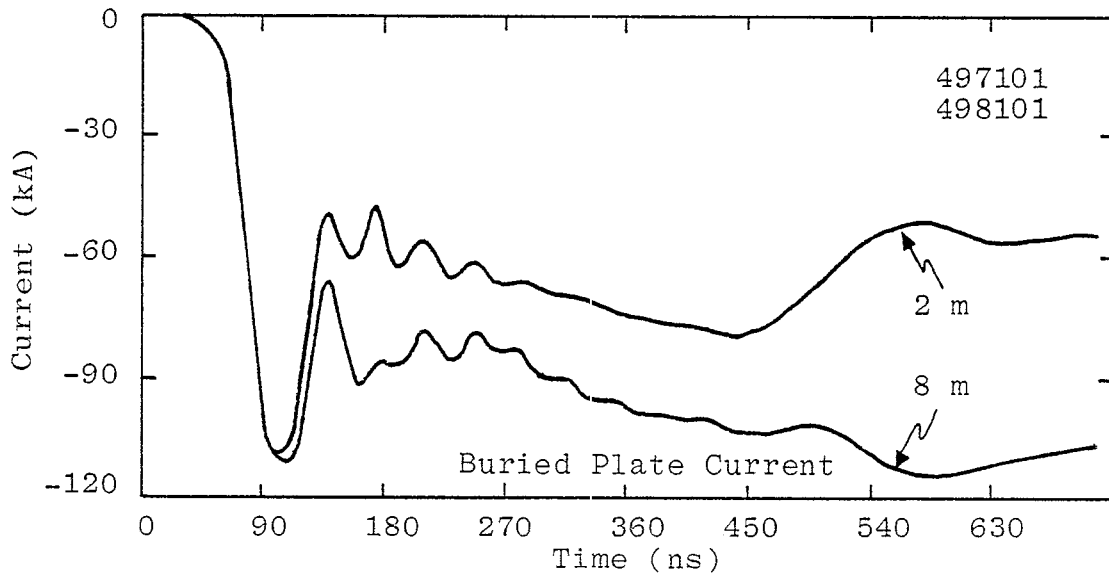
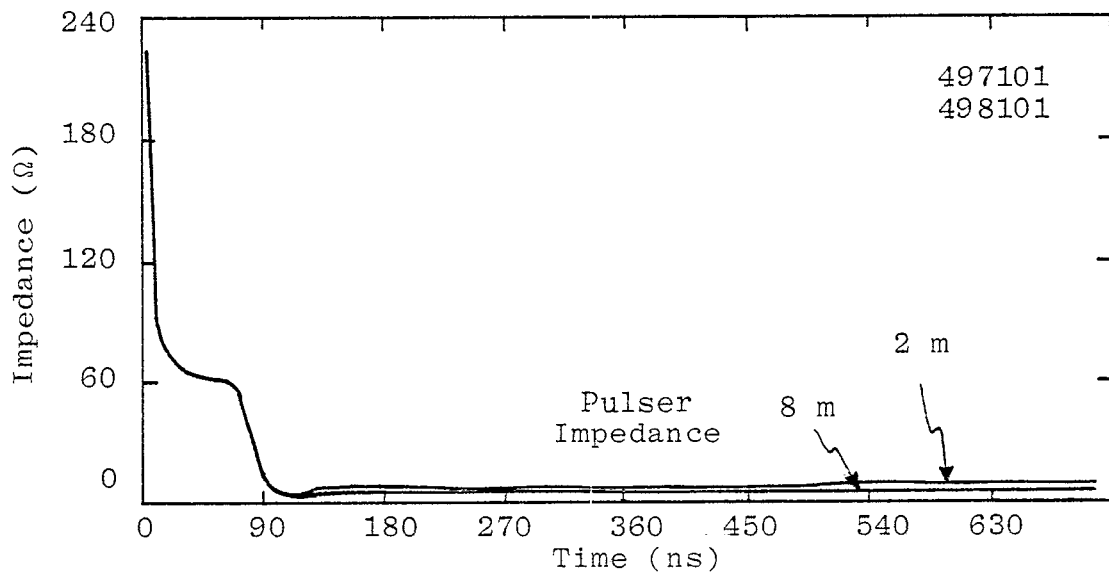
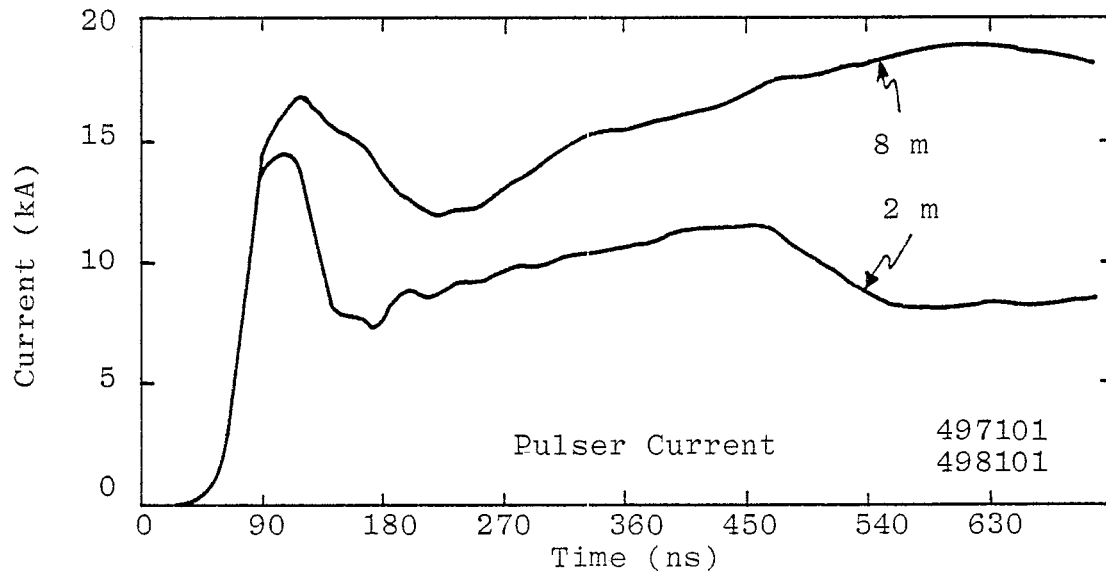


Figure 19. Pulser I, Z and plate I for source end.

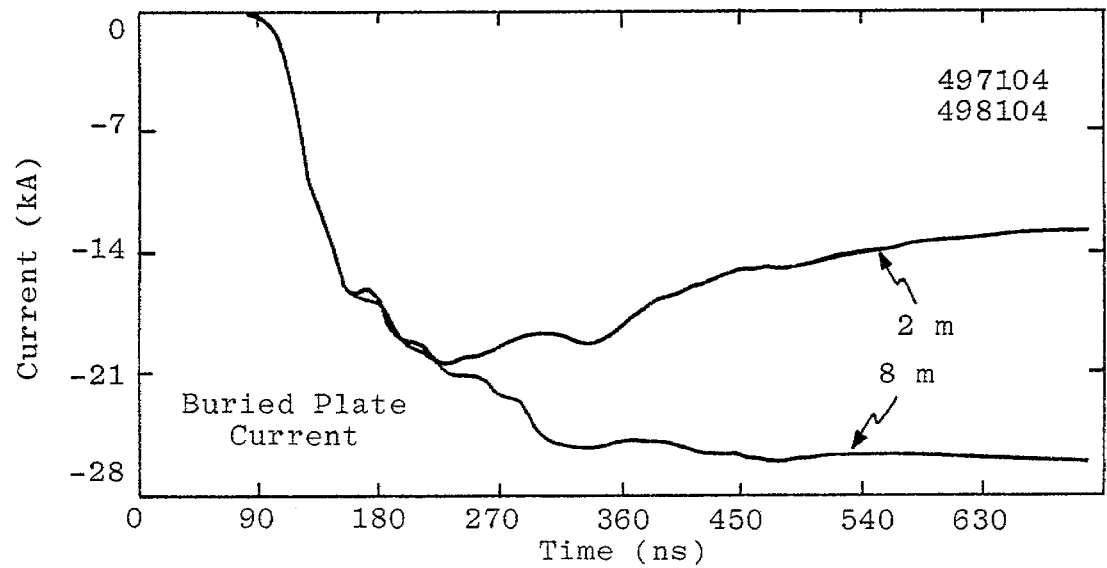
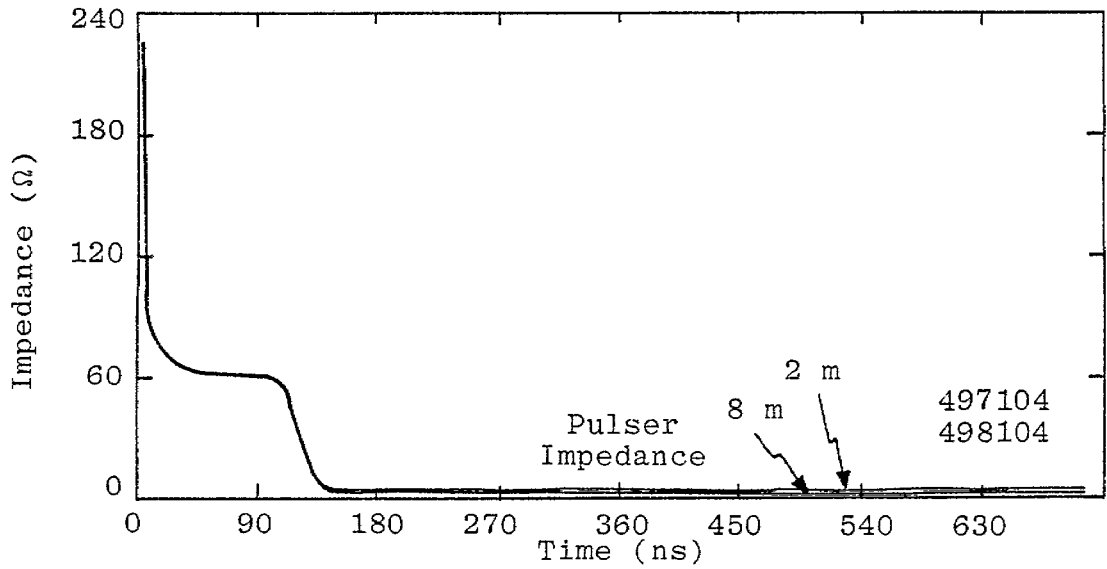
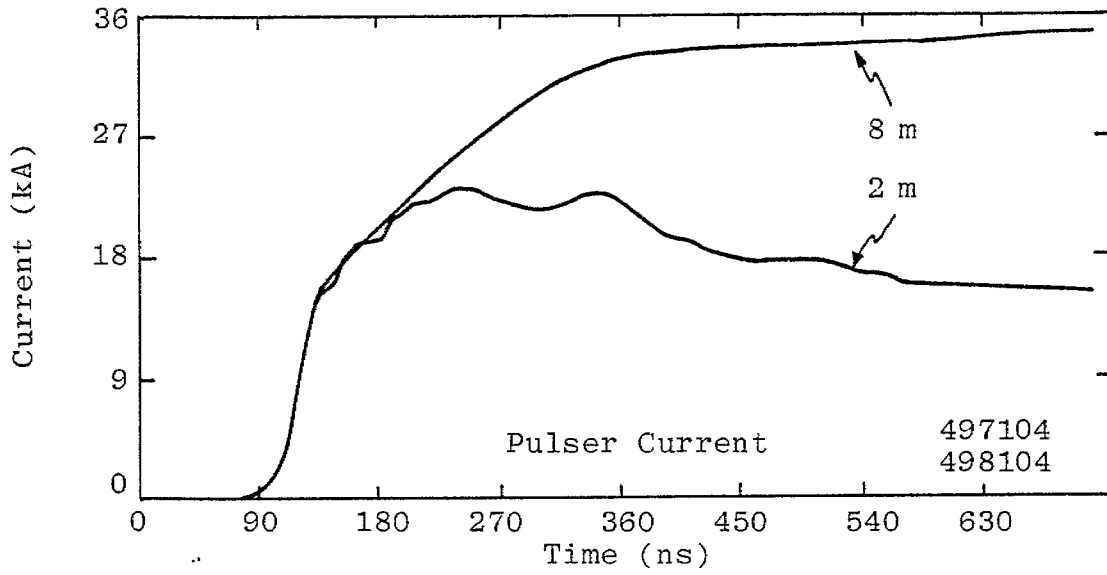


Figure 20. Pulser I, Z and plate I for center location.

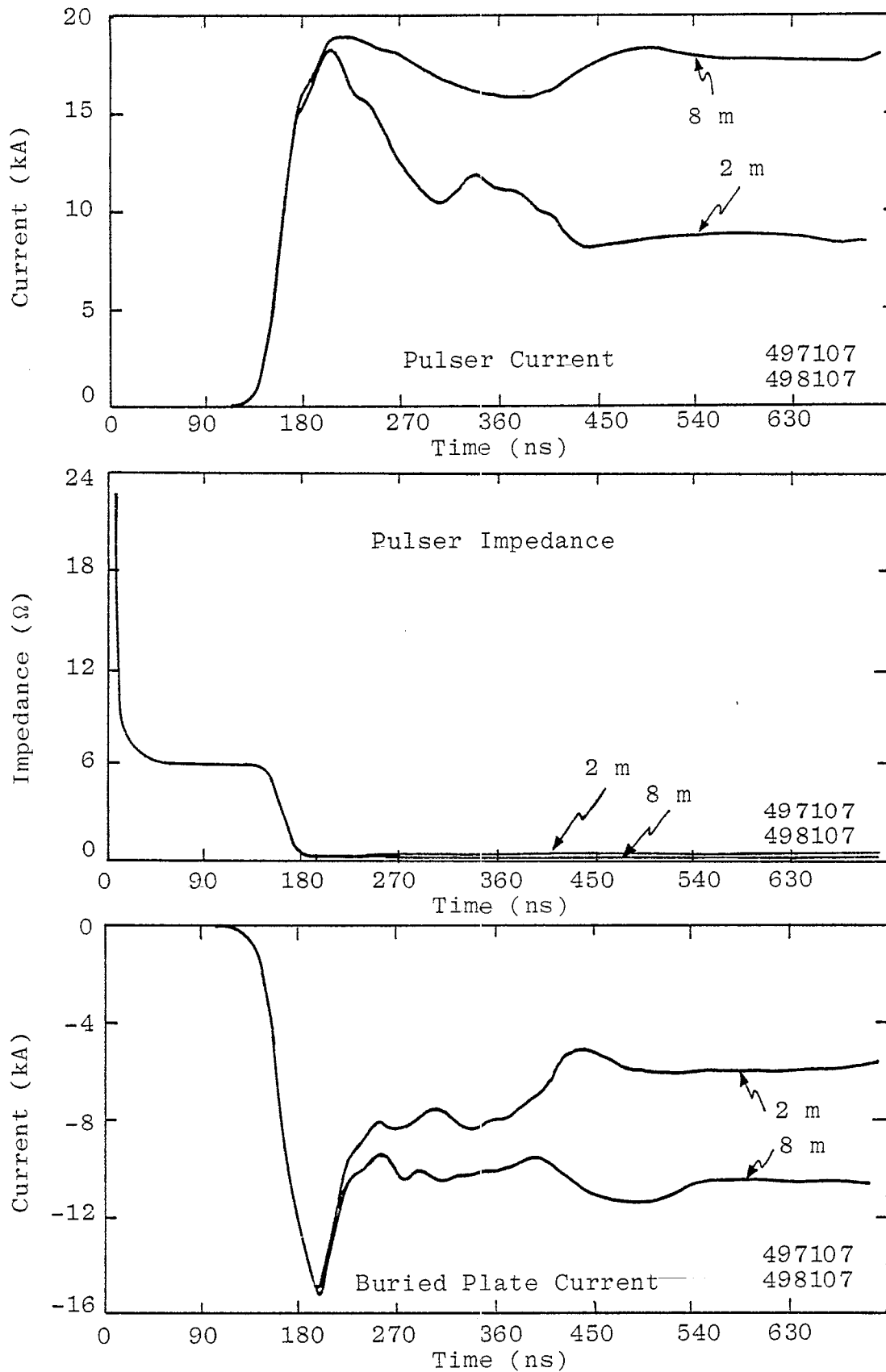


Figure 21. Pulsar I, Z and plate I for far end location.

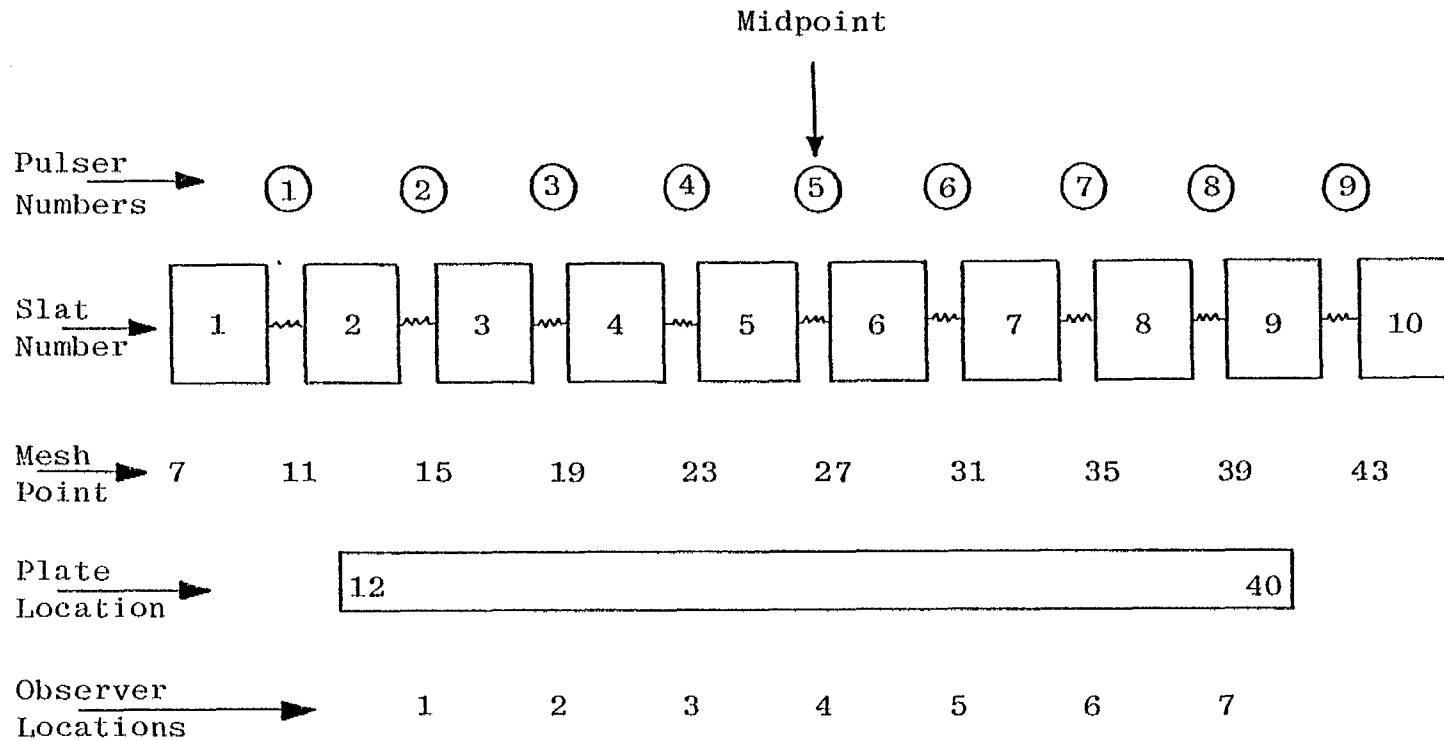


Figure 22. Slat/pulser/plate mesh point locations
 ($\alpha = 1$, $29 \text{ m} \times 4 \text{ m}$ plate, 9 pulsers, $DX = 1$).

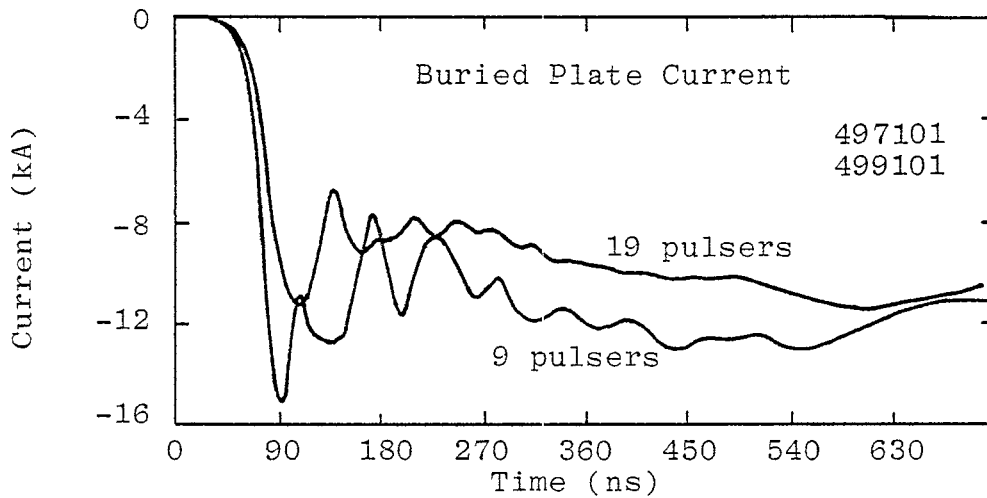
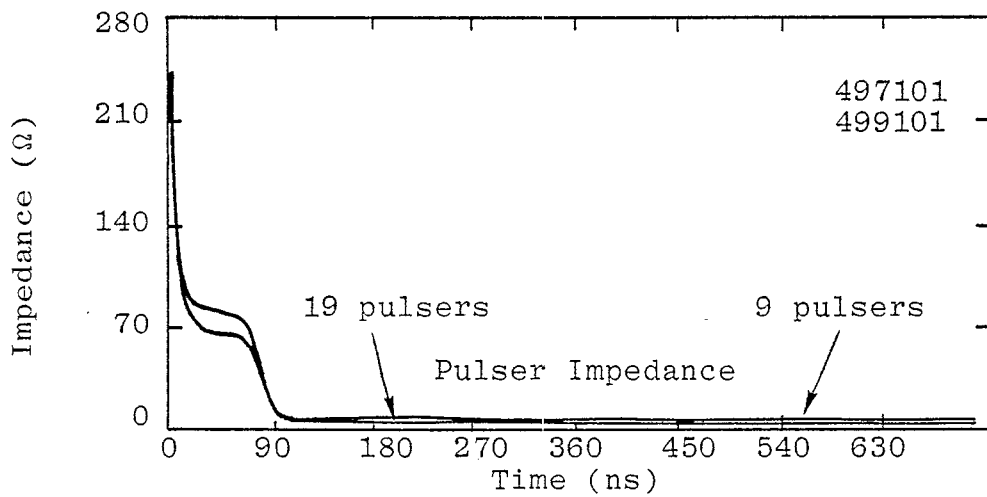
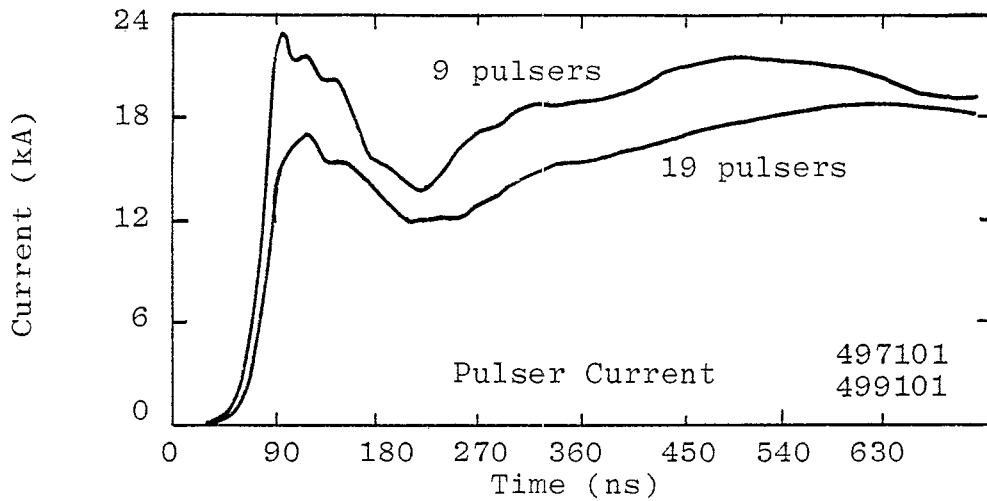


Figure 23. Currents for source end observer 1, for cases $\alpha = 1$, 29 m \times 4 m plate, 8 m slats, DX = 1, 19 pulsers; $\alpha = 1$, 29 m \times 4 m plate, 8 m slats, DX = 1, 9 pulsers.

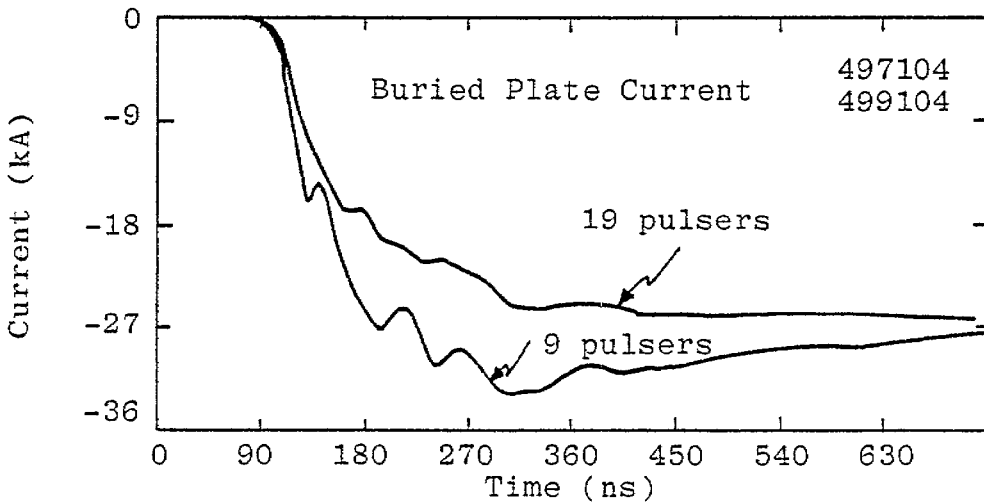
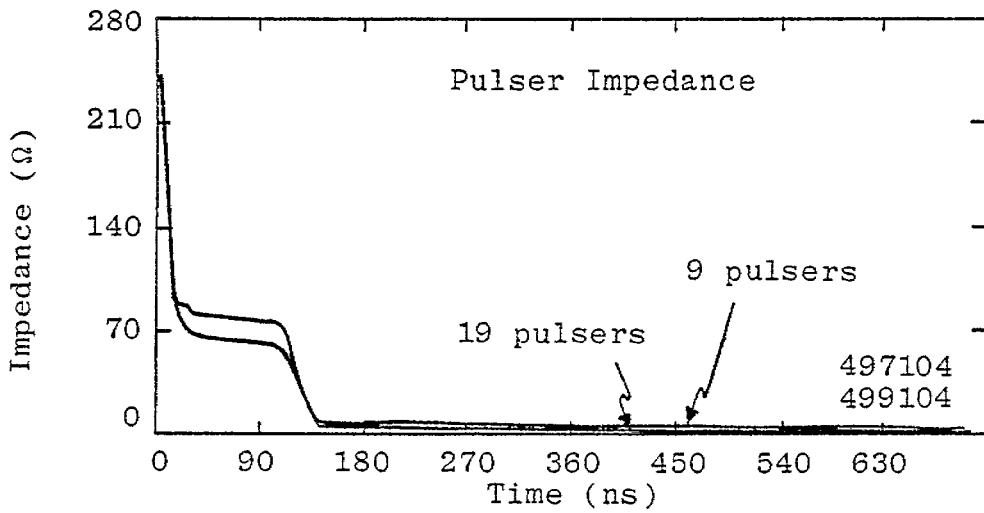
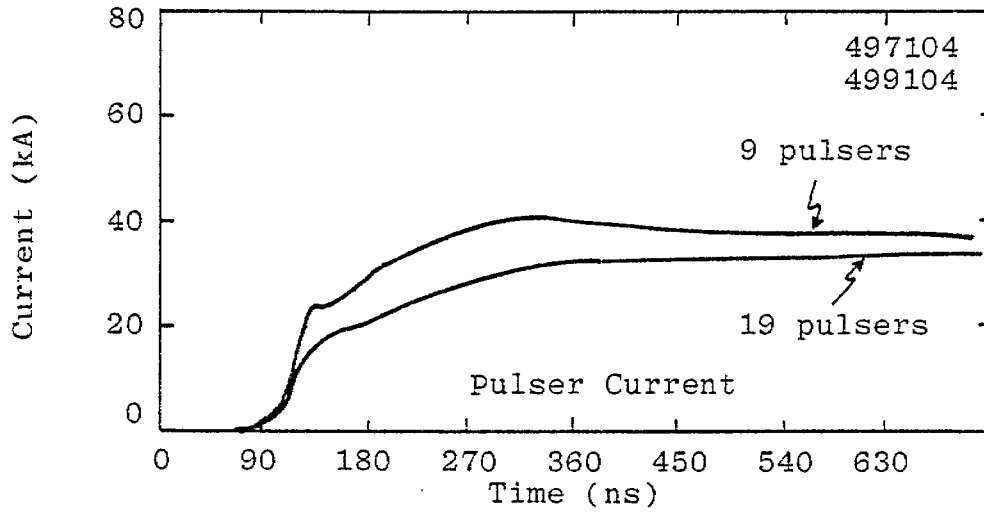
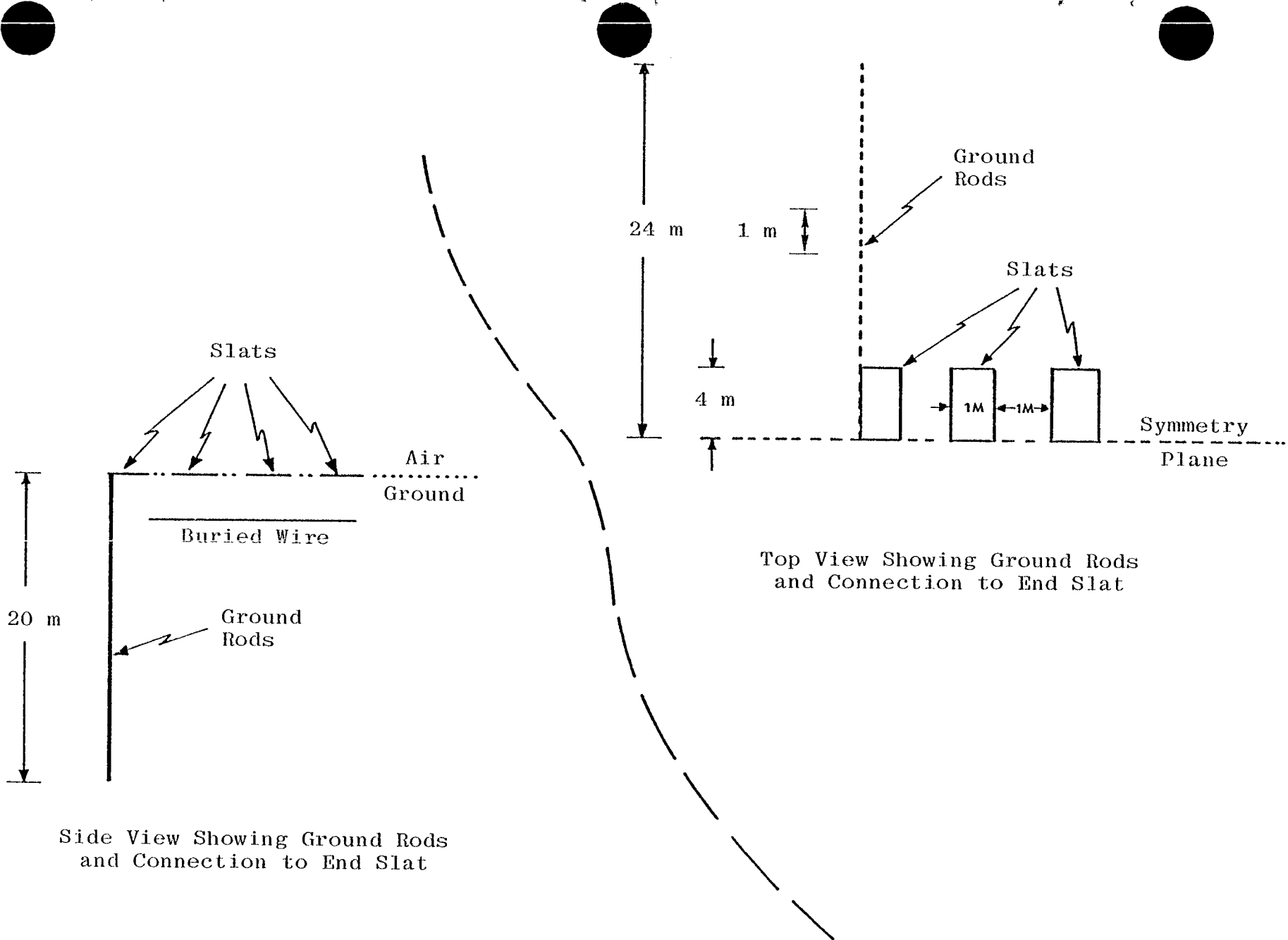


Figure 24. Currents for midpoint observer 4, for cases $\alpha = 1$, $29 \text{ m} \times 4 \text{ m}$ plate, 8 m slats, $\text{DX} = 1$, 19 pulsers; $\alpha = 1$, $29 \text{ m} \times 4 \text{ m}$ plate, 8 m slats, $\text{DX} = 1$, 9 pulsers.



Side View Showing Ground Rods and Connection to End Slat

Top View Showing Ground Rods and Connection to End Slat

Figure 25. Ground rods connected to end plates.

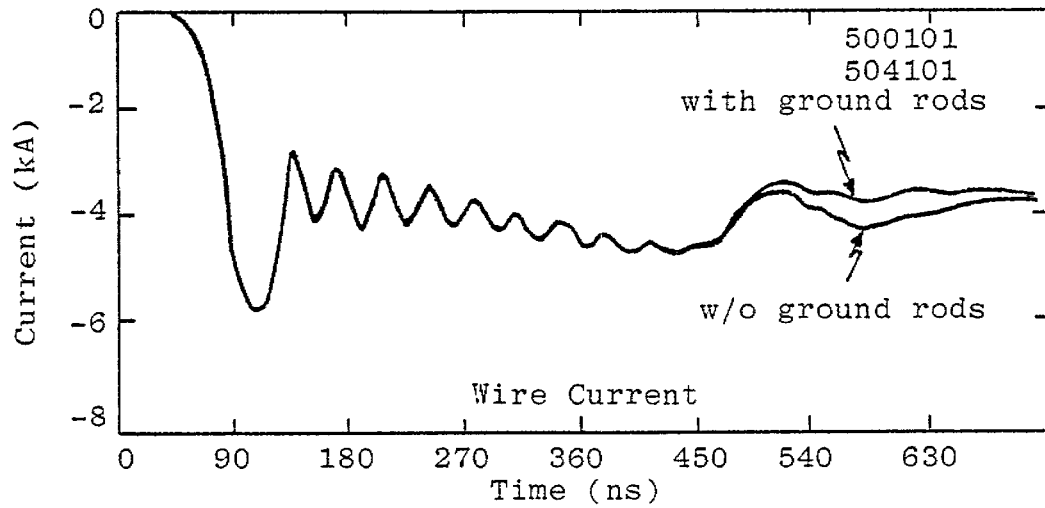
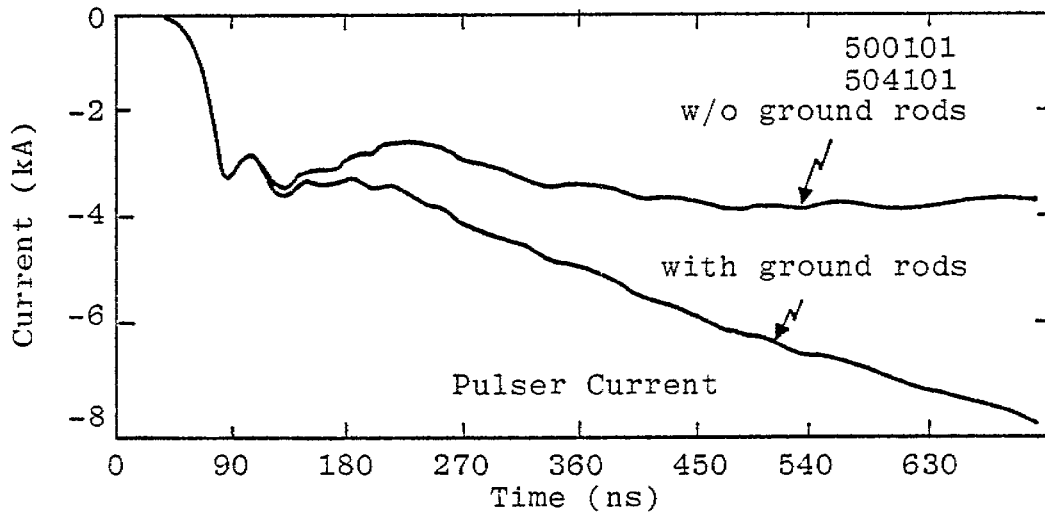


Figure 26. Pulser and wire currents w/wo ground rods (OBS 1, near source).

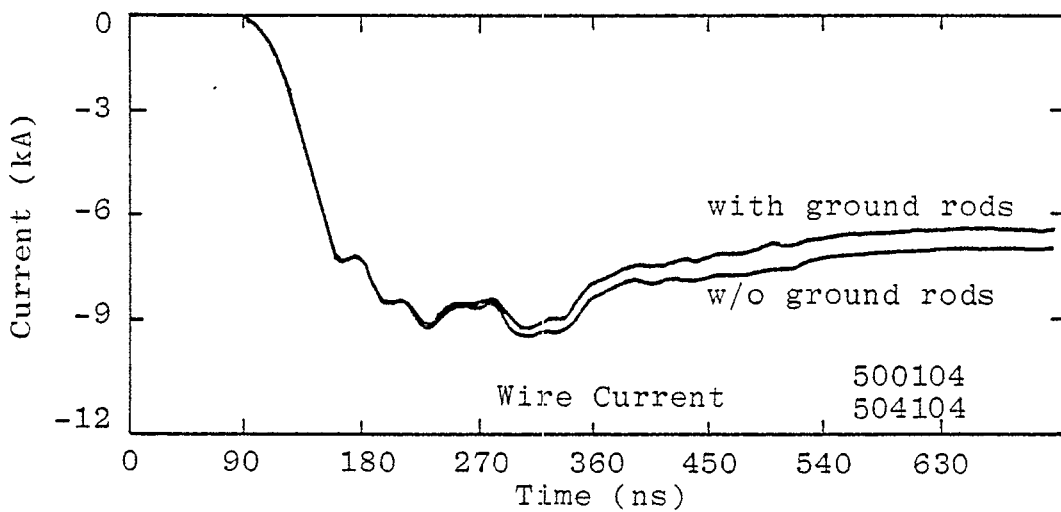
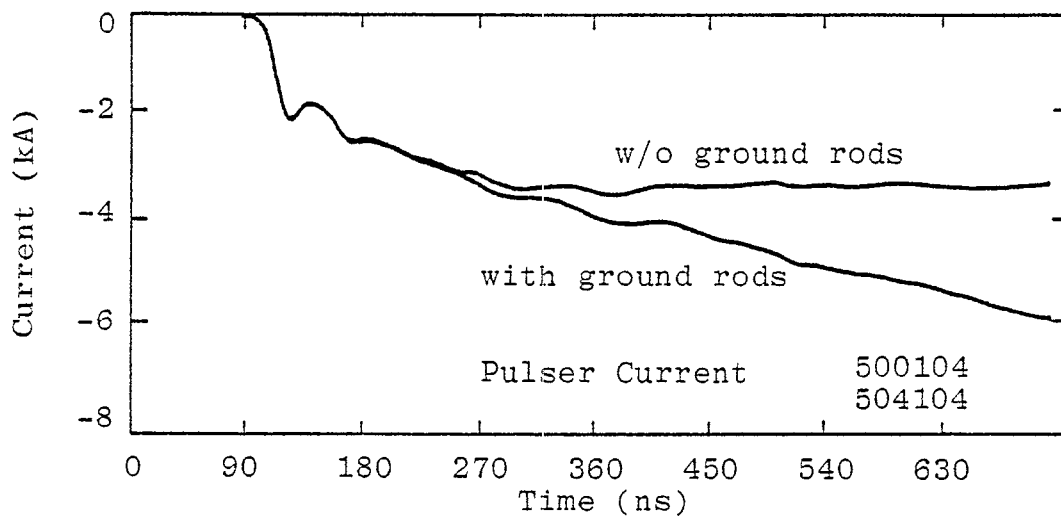


Figure 27. Pulser and wire currents w/o ground rods (OBS 7, far end).

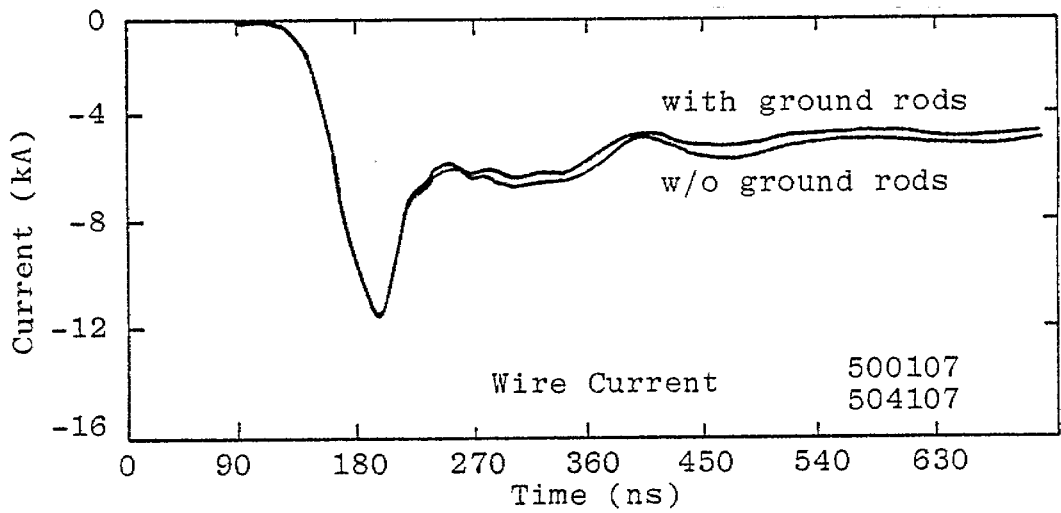
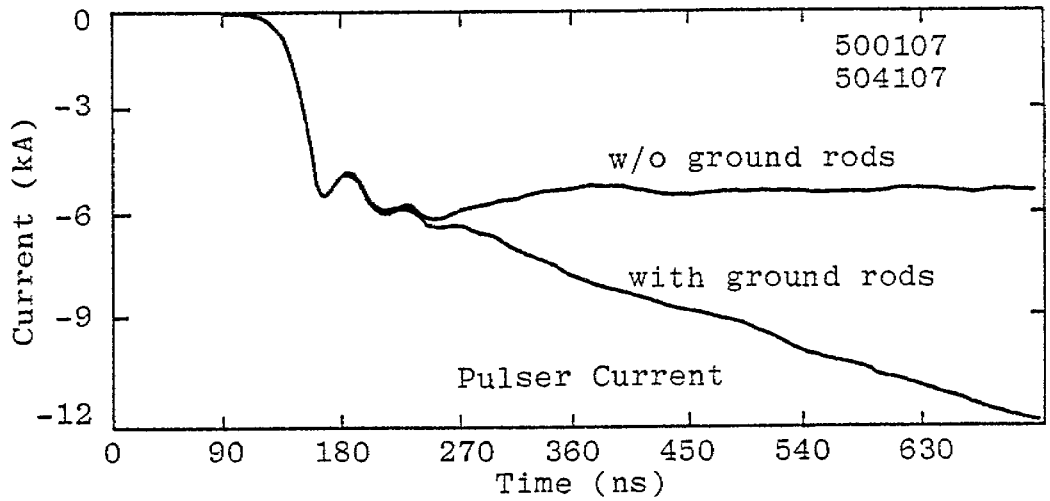


Figure 28. Pulser and wire currents w/wo ground rods (OBS 4, center).

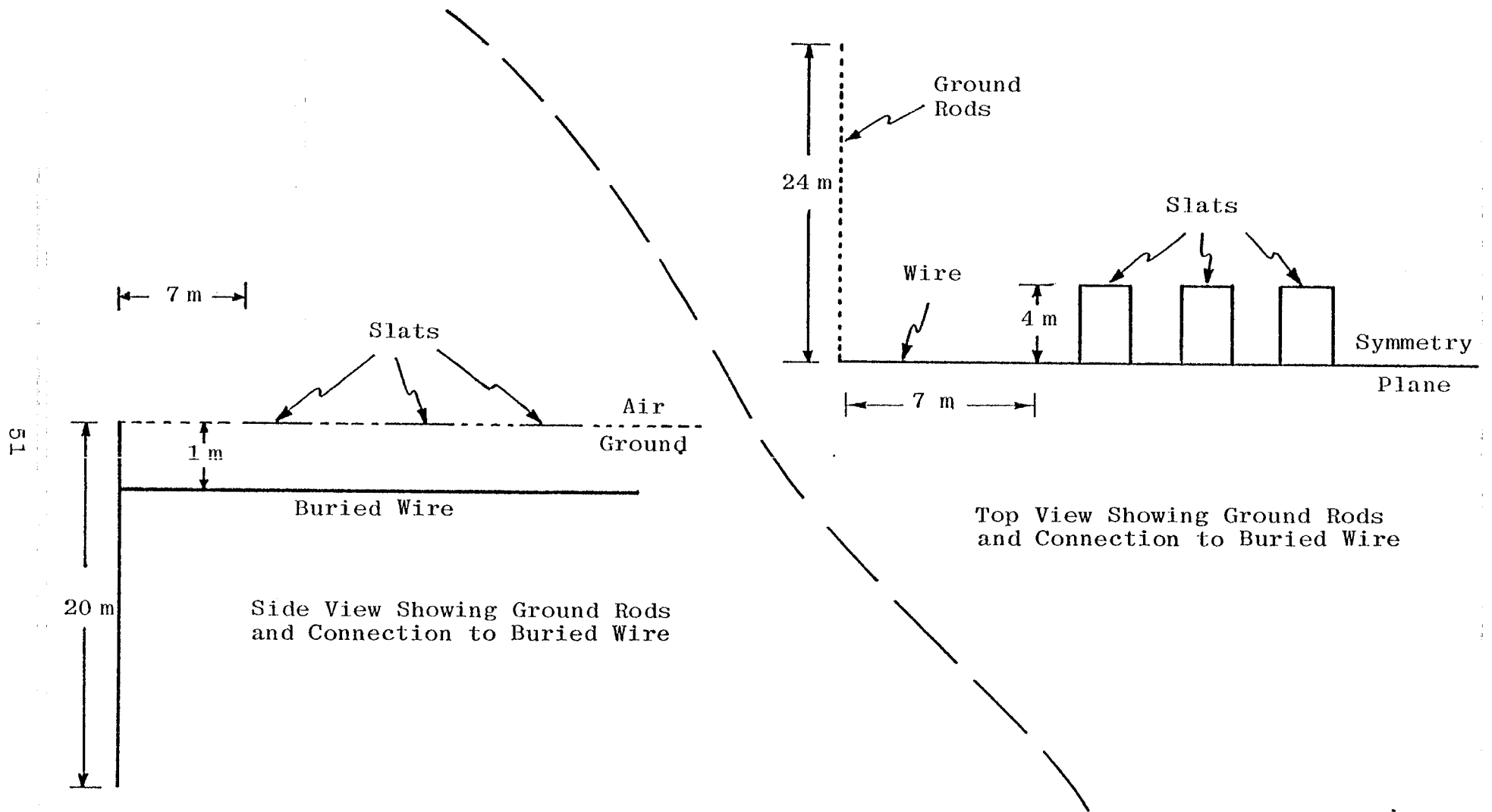


Figure 29. Buried wire connected to ground rods.

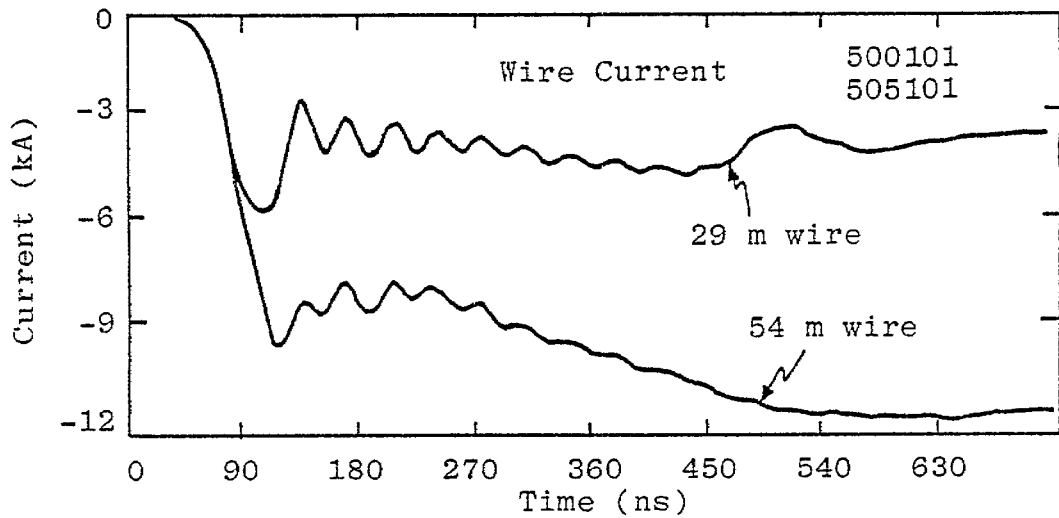
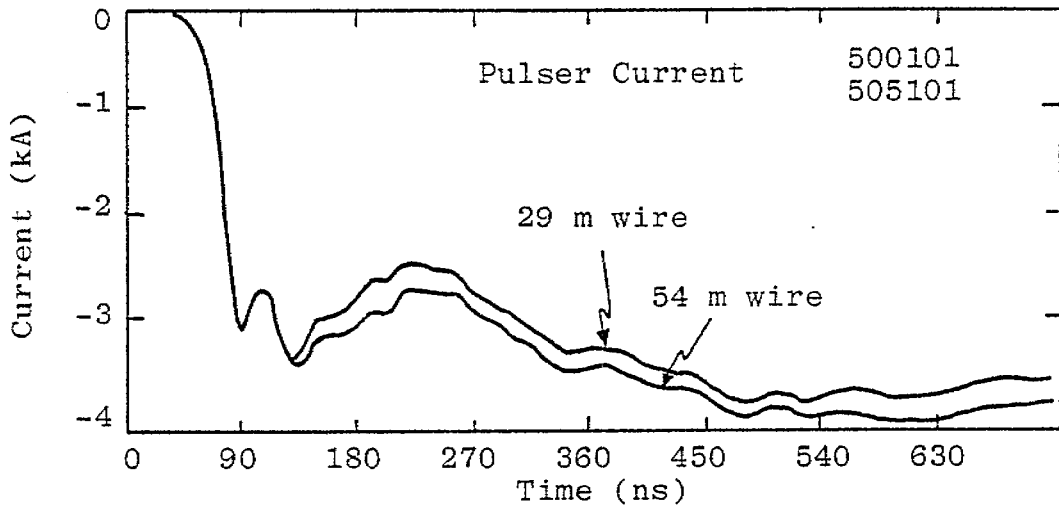


Figure 30. Pulser and wire current for 29 m wire open and 54 m wire shorted to ground rods (OBS 1, near source).

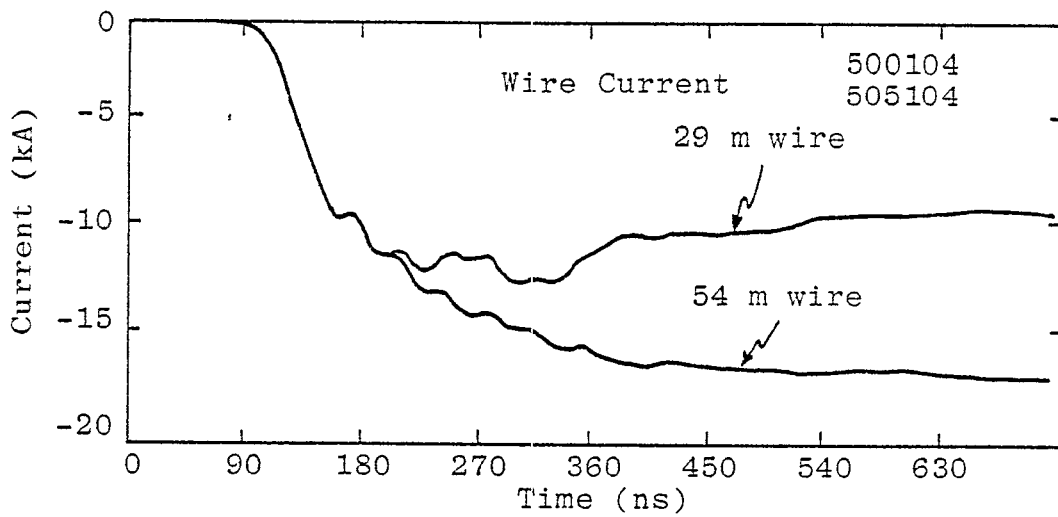
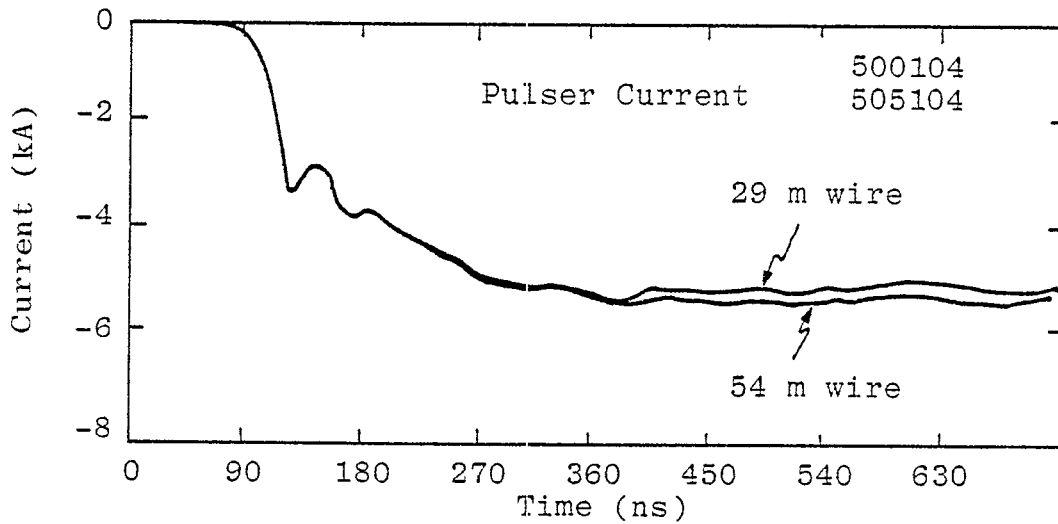


Figure 31. Pulser and wire current for 29 m wire open and 54 m wire shorted to ground rods (OBS 4, center).

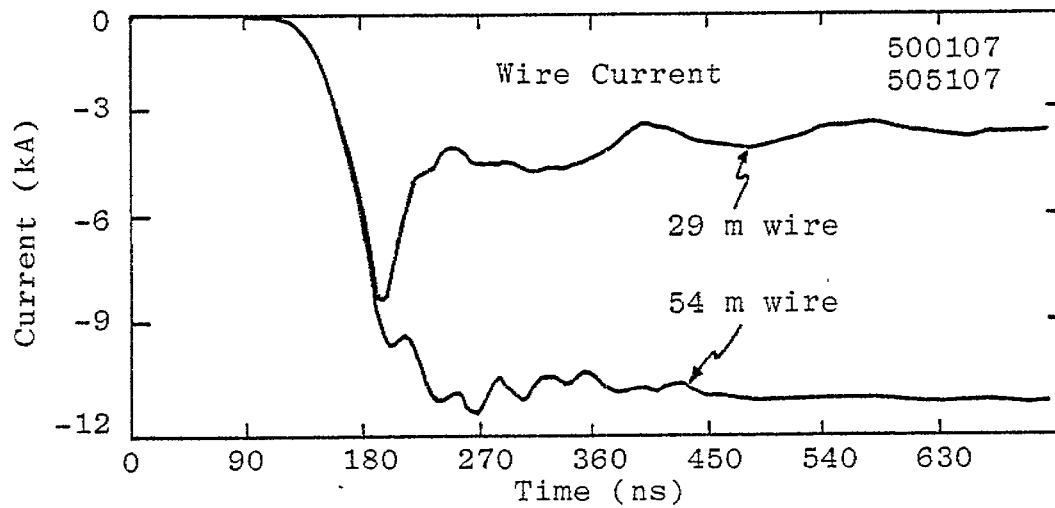
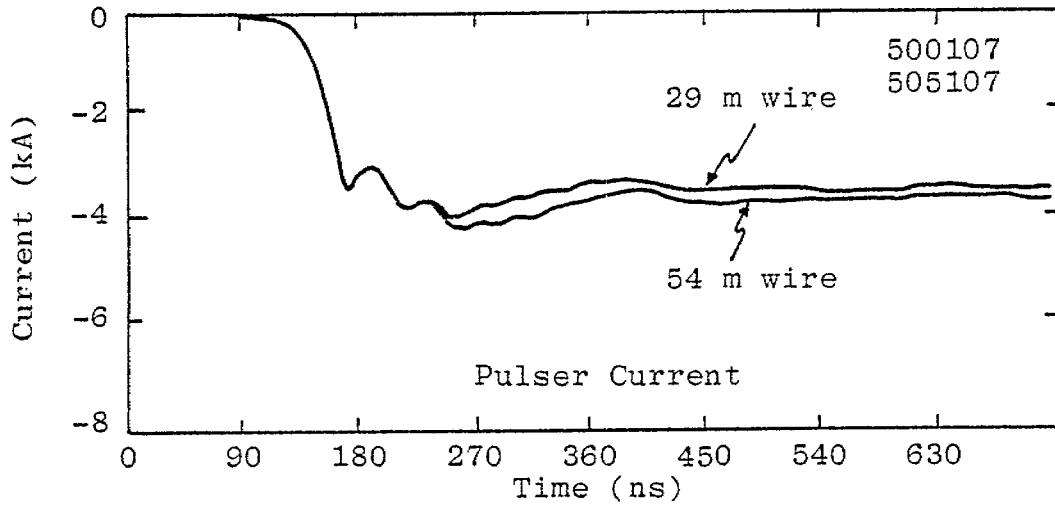
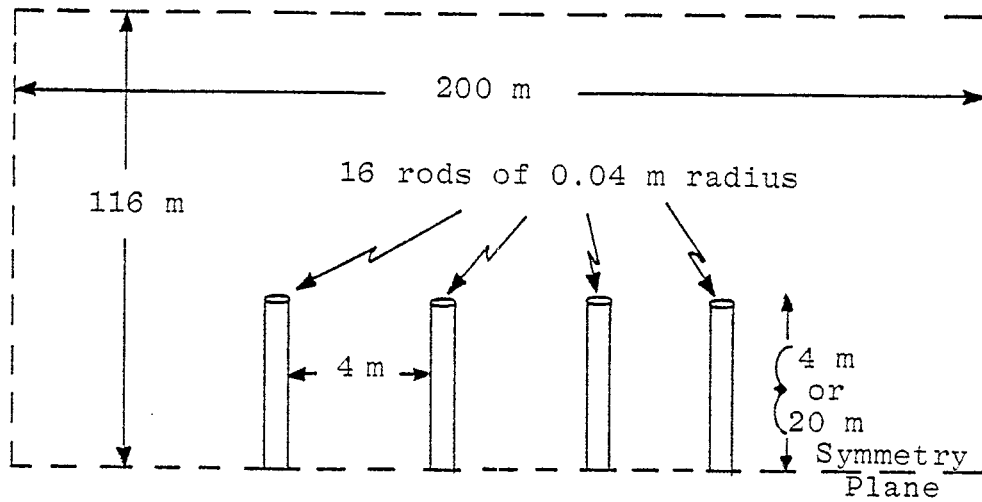
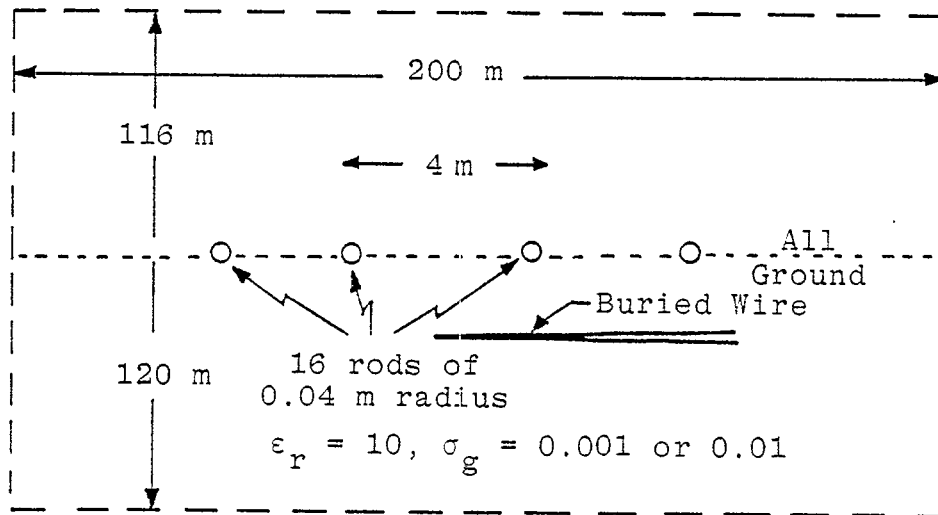


Figure 32. Pulser and wire current for 29 m wire open and 54 m wire shorted to ground rods (OBS 7, far end).



Top View



Side View

Figure 33. Coarse grid geometry for 4 m mesh.

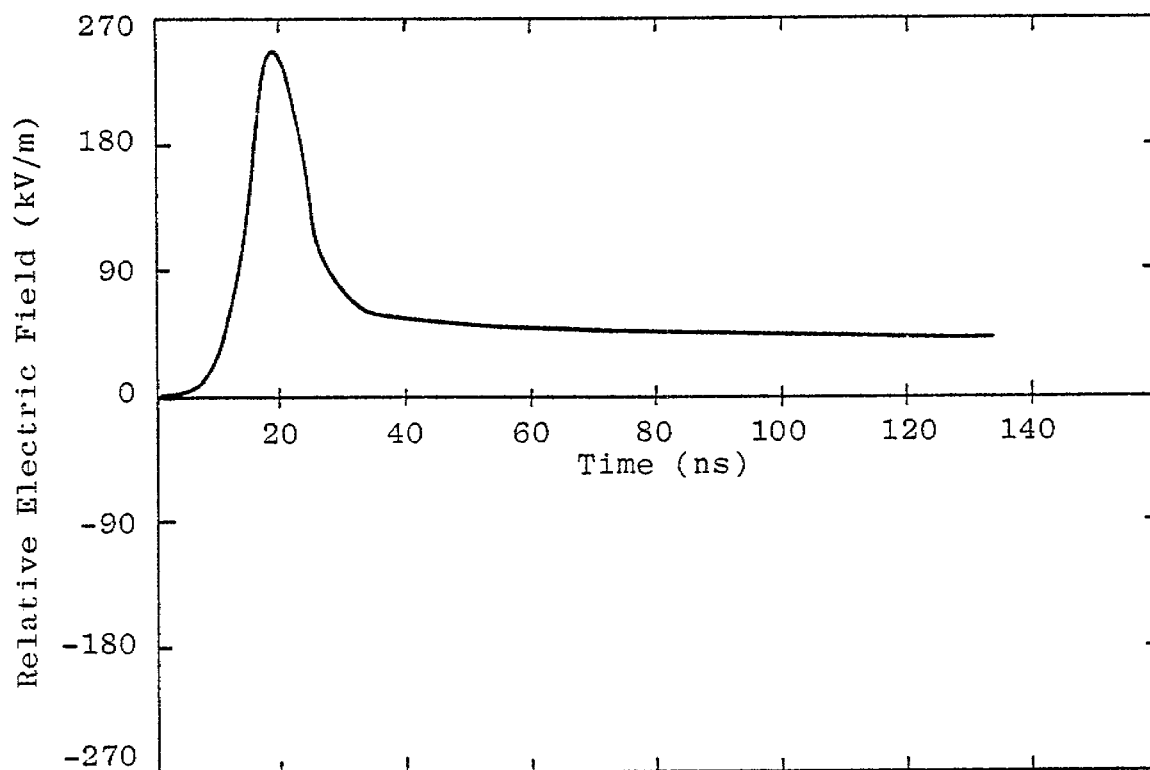


Figure 34. Source voltage for coarse mesh calculations.

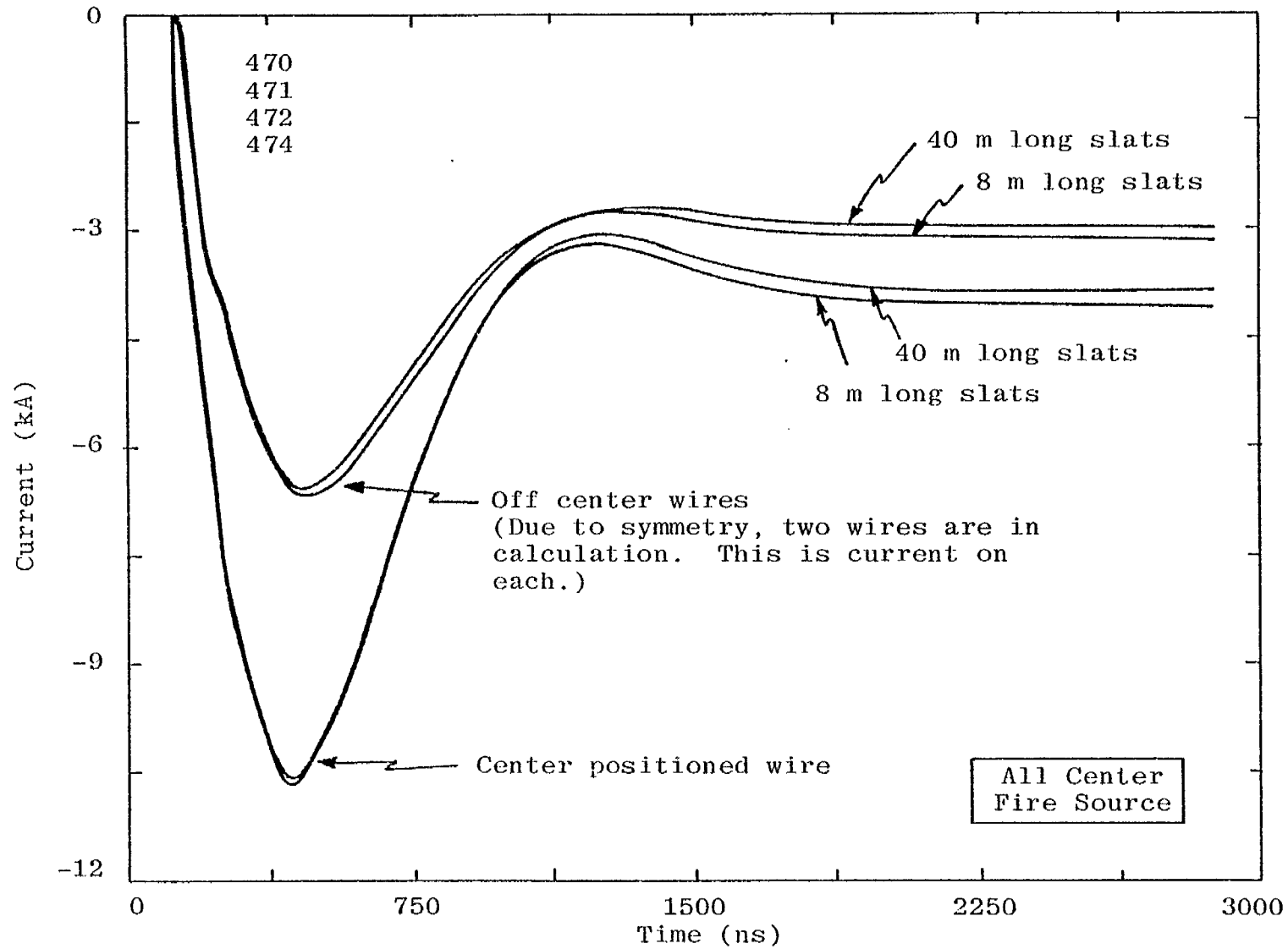


Figure 36. Coarse mesh, 4 m Δ 's, wire currents, 8 m and 40 m long slats, center positioned wire and off center wire.

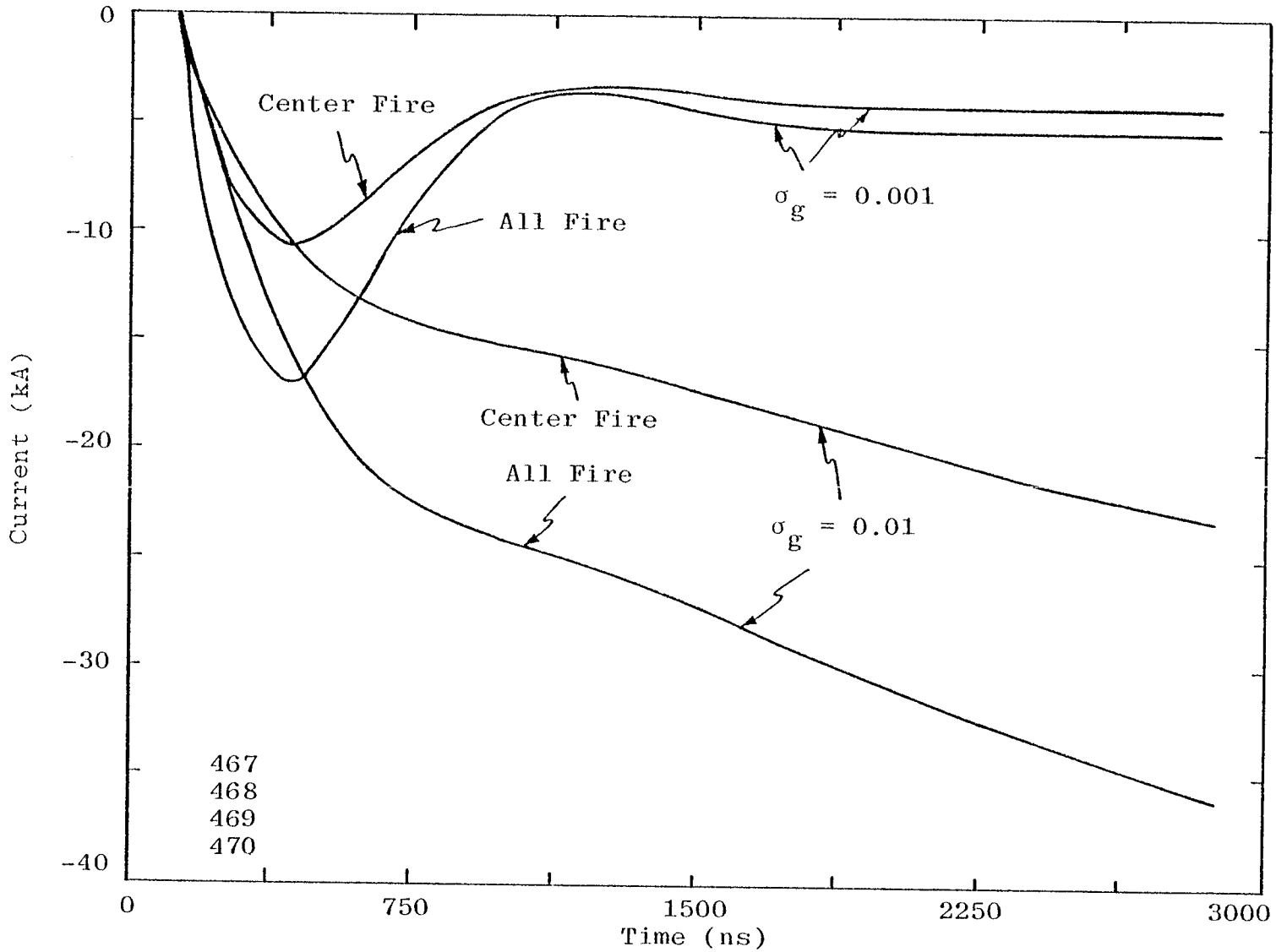


Figure 37. Coarse mesh, 4 m Δ 's, wire currents, 40 m long slats, two ground conductivities (0.001 and 0.01).

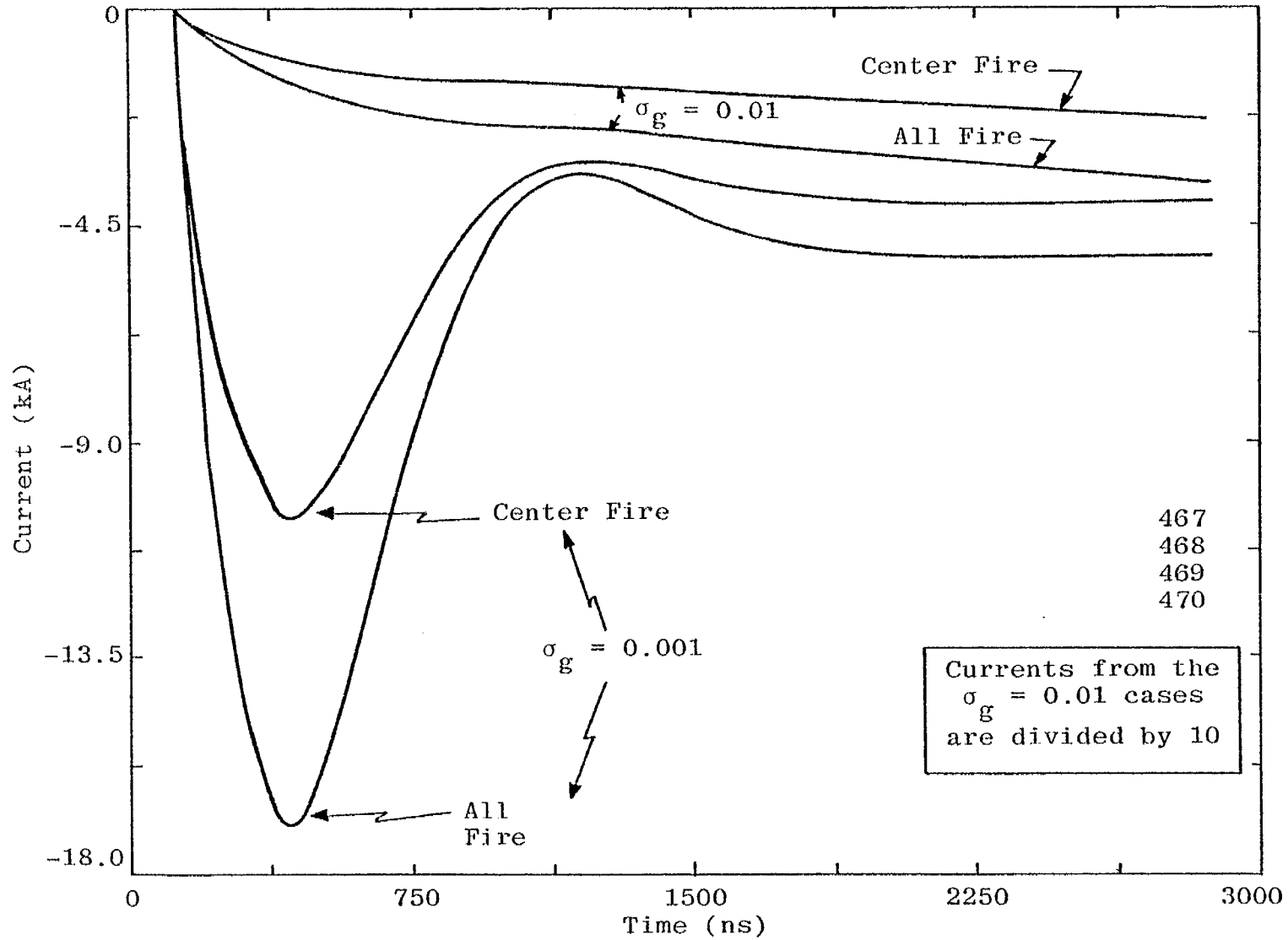


Figure 38. Coarse mesh, 4 m Δ 's, wire currents, 40 m long slats, two ground conductivities (0.001 and 0.01).